

# Event-Triggered Output-Feedback Backstepping Control of Sandwich Hyperbolic PDE Systems

Ji Wang , Member, IEEE, and Miroslav Krstic , Fellow, IEEE

**Abstract**—Motivated by vibration control of a mining cable elevator avoiding frequent actions of a massive actuator, which is a hydraulic cylinder driving a head sheave, we present an event-triggered output-feedback backstepping boundary controller for  $2 \times 2$  coupled hyperbolic partial differential equations (PDEs) sandwiched by two ordinary differential equations (ODEs), through a two-step design including an output-feedback low-pass-filter-based backstepping boundary stabilization law and the subsequent design of a dynamic event-triggering mechanism. The existence of a minimal dwell-time between two triggering times, and exponential convergence in the event-based closed-loop system are proved in this article. In numerical simulations, the proposed control design is validated in the application of axial vibration control of a mining cable elevator.

**Index Terms**—Backstepping, boundary control, distributed parameter system, event-triggered control.

## I. INTRODUCTION

**Motivation:** A mining cable elevator is a vital device used to transport the minerals and miners between thousands of meters underground and the ground surface. Cable plays an indispensable role in the mining elevators due to its advantages of resisting relatively large axial loads and low bending and torsional stiffness, which are helpful to transporting heavy load in large depth. However, a cost to pay for the use of a cable is the appearance of undesirable mechanical vibrations, which lead to premature fatigue fracture, because of the compliance property or the stretching and contracting abilities of cables. Active vibration control is one economic way to suppress vibrations in the long compliant cable because the main structure of the mining elevator does not need to be changed. For example, vibration control forces applied at the head sheave of the mining cable elevator are designed in [44]–[46] based on the PDE model of the mining cable elevator by using backstepping.

When implementing the PDE backstepping laws to practical mining cable elevators, two challenges caused by high-frequency elements in the designed control law appear: 1) the

Manuscript received August 2, 2020; revised November 4, 2020; accepted December 30, 2020. Date of publication January 11, 2021; date of current version December 29, 2021. This work was supported by the National Science Foundation under Grant 1935329 and Grant 1823983. Recommended by Associate Editor Y. Le Gorrec. (Corresponding author: Ji Wang.)

The authors are with the Department of Mechanical and Aerospace Engineering, University of California San Diego, La Jolla, CA 92093-0411 USA (e-mail: jiw248@eng.ucsd.edu; krstic@ucsd.edu).

Color versions of one or more figures in this article are available at <https://doi.org/10.1109/TAC.2021.3050447>.

Digital Object Identifier 10.1109/TAC.2021.3050447

massive actuator consisting of the hydraulic cylinder and head sheave in Fig. 1 is incapable of supporting the fast changing control input because of the low natural frequency. 2) The high-frequency components in the control input may in turn become a vibration source for the cable. It is, thus, required to reduce the actuation frequency and meanwhile ensure the effective suppression of the vibrations in the mining cable elevator.

Designing sampling schemes applied into the control input is a potential solution. Designs of sampled-data control laws of parabolic and hyperbolic partial differential equations (PDEs) were presented in [23], [30] and [12], [31], respectively. Compared with the periodic sampled-data control where unnecessary movements of the massive actuator may exist, event-triggered control where the massive actuator is only animated at the necessary times, which are determined by an event-triggering mechanism of evaluating the operation of the elevator, is more feasible for the mining cable elevator, from the point of view of energy saving.

**Boundary Control of Coupled Hyperbolic PDEs:** Vibration dynamics of a cable with material damping is described as  $2 \times 2$  coupled transport PDEs, converted from wave PDEs with the viscous damping term via Riemann transformation [46]. The boundary control problem of such a system of coupled transport PDEs has been a research focus for the past ten years, with many authors contributing to this topic. Basic boundary stabilization problem of a  $2 \times 2$  coupled linear transport PDEs by backstepping was addressed in [11] and [42]. It was further extended to boundary control of a  $n + 1$  system in [35]. For a more general coupled linear transport PDE system where the number of PDEs in either direction is arbitrary, boundary stabilization law was designed in [17] and [26] by backstepping. Adaptive control for unknown system parameters or disturbance rejection for external periodic disturbances, have been further developed in [4], [5] and [2], [3], [14], [15], respectively.

**Boundary Control of Sandwich PDEs:** Vibration dynamics of the mining cable elevator is described by coupled hyperbolic PDEs sandwiched by two ordinary differential equations (ODEs), which model the cage and the hydraulic actuator dynamics connected with two ends of the mining cable. State-feedback control of a coupled hyperbolic PDE sandwich system was proposed in [8], [9], and [43]. Based on observer designs, output-feedback control of the coupled hyperbolic PDE sandwich system was designed in [16], [37], and [48]. The boundary control designs of sandwich systems containing other type PDEs were also proposed in [6], [27], and [28] (transport PDE), [32] (viscous Burgers PDE), and [47] (heat PDE).

**Event-Triggered Control:** An event-triggering mechanism is to be designed to reduce the actuation frequency of the control

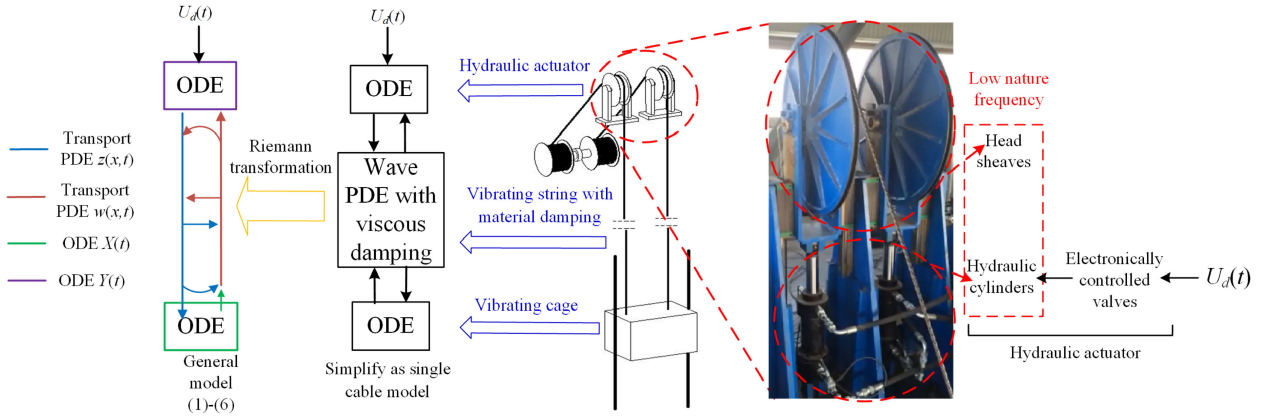


Fig. 1. Relationship between the sandwich hyperbolic PDE system and the mining cable elevators consisting of hydraulic-driven head sheave, mining cable, and cage.

input while ensure the effective vibration suppression. Most of current designs of the event-triggering mechanism (ETM) are for ODE systems, such as [24], [25], [33], [40], [41]. There are few studies about event-based control of PDE systems. Selivanov and Fridman [39] and Yao and El-Farra [50] proposed event-triggered control schemes for distributed (in-domain) control of PDEs. For the boundary control of PDEs, an event-triggered control law was originally proposed in [18] and [19] for hyperbolic PDEs with dissipativity boundary conditions. Afterwards, event-triggered boundary control of reaction-diffusion PDEs was also dealt with in [21]. In the meantime, a state-feedback event-based boundary controller of  $2 \times 2$  coupled linear hyperbolic PDEs without a proximal reflection term at the boundary was first proposed in [20]. Incorporating this proximal reflection term, observer-based event-triggered boundary control of  $2 \times 2$  coupled linear hyperbolic PDEs was further developed in [22], which assumed that the product of the proximal and distal reflection gains is smaller than one-half and the proximal reflection term was completely preserved in the closed-loop system. For the mining cable elevator model, this assumption is required to be relieved and the proximal reflection term at the PDE boundary needs to be cancelled completely or partially via design of an event-triggered control input acting at an ODE in the input channel of the PDE, which makes the design and analysis of the event-based closed-loop system challenging.

#### Contributions of this article.

- 1) Compared with [20], [22], which designed an event-triggered backstepping controller for  $2 \times 2$  hyperbolic PDEs, in this article, besides two additional ODEs, the restriction on the proximal and distal reflection gains in  $2 \times 2$  hyperbolic PDEs is relieved and the proximal reflection term is compensated by the event-based control law which goes through the input ODE, which is stabilized meanwhile.
- 2) In comparison to the recent results about exponential stabilization of sandwich hyperbolic systems [8], [16], [37], [43], [49] by continuous-in-time control laws, this article achieves exponential convergence through an event-based control law. This is the first result of event-triggered backstepping boundary control of sandwich PDE systems.

- 3) To the best of our knowledge, this is also the first result of applying the event-triggered scheme in vibration control of PDE-modeled string-payload vibrating systems, which physically describe elevators, cranes, etc.

*Organization:* The rest of this article is organized as follows. The concerned model is described in Section II. A state observer is designed in Section III. A low-pass-filter-based backstepping output-feedback boundary controller is presented in Section IV. The event-triggering mechanism is designed and the existence of a minimal dwell-time between two triggering times is proved in Section V. The achievement of exponential convergence in the event-based closed-loop system is proved via Lyapunov analysis in Section VI. The controller is applied into axial vibration control of a mining cable elevator in Section VII. The conclusion and future work are provided in Section VIII.

*Notation:* We adopt the following notation. The symbol  $R^-$  denotes the set of negative real numbers, whose complement on the real axis is  $\mathbb{R}_+ := [0, +\infty)$ . For an interval  $\bar{U} \subseteq \mathbb{R}_+$  and a set  $\bar{\Omega} \subseteq \mathbb{R}$ , by  $C^0(\bar{U}; \bar{\Omega})$ , we denote the class of continuous mappings on  $\bar{U}$ , which take values in  $\bar{\Omega}$ . We use the notation  $L^2(0, 1)$  for the standard space of the equivalence class of square-integrable, measurable functions defined on  $(0, 1)$  and  $\|f\| = ( \int_0^1 f(x)^2 dx )^{\frac{1}{2}} < +\infty$  for  $f \in L^2(0, 1)$ . For an integer  $k \geq 1$ ,  $H^k(0, 1)$  denotes the Sobolev space of functions in  $L^2(0, 1)$  with all its weak derivatives up to order  $k$  in  $L^2(0, 1)$ . The usual Euclidean norm is denoted by  $|\cdot|$ . For an interval  $I \subseteq \mathbb{R}_+$ , the space  $C^0(I; L^2(0, 1))$  is the space of continuous mappings  $I \ni t \mapsto u(x, t) \in L^2(0, 1)$ .

## II. PROBLEM FORMULATION

The plant considered in this article is

$$\dot{Y}(t) = A_0 Y(t) + E_0 w(0, t) + B_0 U(t) \quad (1)$$

$$z(0, t) = p w(0, t) + C_0 Y(t) \quad (2)$$

$$z_t(x, t) = -q_1 z_x(x, t) - c_1 w(x, t) - c_1 z(x, t) \quad (3)$$

$$w_t(x, t) = -q_2 w_x(x, t) - c_2 w(x, t) - c_2 z(x, t) \quad (4)$$

$$w(1, t) = q z(1, t) + C X(t) \quad (5)$$

$$\dot{X}(t) = A X(t) + B z(1, t) \quad (6)$$

$\forall(x, t) \in [0, 1] \times [0, \infty)$ . The vector  $Y(t) \in \mathbb{R}^{\bar{n} \times 1}$ ,  $X(t) \in \mathbb{R}^{n \times 1}$  are ODE states, where positive constants  $\bar{n}, n$  are the dimensions of two ODEs. The scalars  $z(x, t) \in \mathbb{R}, w(x, t) \in \mathbb{R}$  are the states of the  $2 \times 2$  coupled hyperbolic PDEs. The positive constants  $q_1$  and  $q_2$  are the transport velocities. The constants  $c_1, c_2$  are arbitrary and  $p, q$  satisfy Assumption 3 shown below. The vector  $E_0 \in \mathbb{R}^{\bar{n} \times 1}$  is arbitrary. The control input  $U(t) \in \mathbb{R}$  is to be designed. The plant initial conditions are taken as  $(Y(0), z(x, 0), w(x, 0), X(0)) \in \chi = \mathbb{R}^{\bar{n}} \times H^{n_r+1}(0, 1)^2 \times \mathbb{R}^n$  where  $n_r$  is the relative degree of (1). The matrices in the ODE subsystems  $A \in \mathbb{R}^{n \times n}$ ,  $A_0 \in \mathbb{R}^{\bar{n} \times \bar{n}}$ ,  $B \in \mathbb{R}^{n \times 1}$ ,  $B_0 \in \mathbb{R}^{\bar{n} \times 1}$ ,  $C \in \mathbb{R}^{1 \times n}$ ,  $C_0 \in \mathbb{R}^{1 \times \bar{n}}$  are subject to Assumptions 1 and 2.

*Assumption 1:* The pairs  $(A, B)$  and  $(A_0, B_0)$  are controllable. The pairs  $(A, C)$  and  $(A_0, C_0)$  are observable.

Based on this assumption, there exist constant matrices  $K, L, K_0, L_0$  to make the following matrices Hurwitz:

$$\hat{A} = A - BK \quad (7)$$

$$\bar{A} = A - LC \quad (8)$$

$$\hat{A}_0 = A_0 - B_0 K_0 \quad (9)$$

$$\bar{A}_0 = A_0 - L_0 C_0. \quad (10)$$

The following assumption for the ODE in the input channel ensures a stable left inversion of the system  $(A_0, B_0, C_0)$  [34].

*Assumption 2:*  $(C_0, A_0, B_0)$  satisfy

$$\det\left(\begin{bmatrix} sI - A_0 & B_0 \\ C_0 & 0 \end{bmatrix}\right) \neq 0 \quad (11)$$

for all  $s \in \mathbb{C}, \Re(s) \geq 0$ .

The following assumption about the PDE subsystem parameters, which will be used in the low-pass filter design, are satisfied in the mining cable elevator model.

*Assumption 3:* The plant parameters  $p, q$  satisfy  $|pq|e^{\left(\frac{c_2}{q_2} + \frac{c_1}{q_1}\right)} < 1$  and  $q \neq 0$ .

The control objective of this article is to exponentially stabilize (1)–(6) by designing an event-triggered boundary control input using only a collocated measurement  $w(0, t)$ .

It is shown in Fig. 1 that axial vibration dynamics of the mining cable elevator consisting of the hydraulic actuator, mining cable, and cage is described by a sandwich wave PDE system. It is also shown in the figure that this system can be transformed, using a Riemann transformation, into a  $2 \times 2$  coupled transport PDE sandwich system, considered in this article, and for which Assumptions 1–3 are satisfied. A specific wave PDE-modeled mining cable elevator, the physical meaning of the states and parameters, and the according transformation to the considered plant (1)–(6), are shown in Section VII.

### III. OBSERVER

In order to estimate the distributed states, which usually cannot be measured but are required in the controller, a state observer for the plant (1)–(6) is designed in this section using only the measurement  $w(0, t)$  at the actuated boundary, i.e., using only the sensing of signals at the head sheaves of the mining cable elevator. The observer is postulated with the same structure as in [16], namely, as follows:

$$\dot{\hat{Y}}(t) = A_0 \hat{Y}(t) + E_0 w(0, t) + B_0 U(t)$$

$$+ \Psi_0(w(0, t) - \hat{w}(0, t)) \quad (12)$$

$$\hat{z}(0, t) = pw(0, t) + C_0 \hat{Y}(t) \quad (13)$$

$$\begin{aligned} \hat{z}_t(x, t) = & -q_1 \hat{z}_x(x, t) - c_1 \hat{w}(x, t) - c_1 \hat{z}(x, t) \\ & + \Psi_1(x)(w(0, t) - \hat{w}(0, t)) \end{aligned} \quad (14)$$

$$\begin{aligned} \hat{w}_t(x, t) = & q_2 \hat{w}_x(x, t) - c_2 \hat{w}(x, t) - c_2 \hat{z}(x, t) \\ & + \Psi_2(x)(w(0, t) - \hat{w}(0, t)) \end{aligned} \quad (15)$$

$$\hat{w}(1, t) = q \hat{z}(1, t) + C \hat{X}(t) \quad (16)$$

$$\dot{\hat{X}}(t) = A \hat{X}(t) + B \hat{z}(1, t) + \Psi_3(w(0, t) - \hat{w}(0, t)) \quad (17)$$

where  $\Psi_0, \Psi_1(x), \Psi_2(x), \Psi_3$  are observer gains to be determined. The control input  $U(t)$  can be replaced by an event-triggered control law  $U_d(t)$  presented later in the event-based closed-loop system.

Define observer error states as

$$\begin{aligned} & [\tilde{z}(x, t), \tilde{w}(x, t), \tilde{X}(t), \tilde{Y}(t)] \\ & = [z(x, t), w(x, t), X(t), Y(t)] - [\hat{z}(x, t), \hat{w}(x, t), \hat{X}(t), \hat{Y}(t)]. \end{aligned} \quad (18)$$

Apply the backstepping transformation

$$\begin{aligned} \tilde{z}(x, t) = & \tilde{\alpha}(x, t) - \int_0^x \bar{\phi}(x, y) \tilde{\alpha}(y, t) dy \\ & - \int_0^x \bar{\phi}_1(x, y) \tilde{\beta}(y, t) dy - \bar{\gamma}(x) \tilde{Y}(t) \end{aligned} \quad (19)$$

$$\begin{aligned} \tilde{w}(x, t) = & \tilde{\beta}(x, t) - \int_0^x \bar{\psi}(x, y) \tilde{\alpha}(y, t) dy \\ & - \int_0^x \bar{\psi}_1(x, y) \tilde{\beta}(y, t) dy - \bar{\varphi}(x) \tilde{Y}(t) \end{aligned} \quad (20)$$

and

$$\tilde{Z}(t) = \tilde{X}(t) - \int_0^1 K_1(y) \tilde{\alpha}(y, t) dy - \int_0^1 K_2(y) \tilde{\beta}(y, t) dy \quad (21)$$

where the conditions, which are well-posed, on the functions  $\bar{\phi}, \bar{\phi}_1, \bar{\psi}, \bar{\psi}_1, \bar{\gamma}, \bar{\varphi}, K_1, K_2$  are given in (A.1)–(A.16) in the Appendix. The observer error system- $(\tilde{z}, \tilde{w}, \tilde{X}, \tilde{Y})$  can be converted to an exponentially stable target observer error system as follows:

$$\tilde{\alpha}(0, t) = 0 \quad (22)$$

$$\tilde{\alpha}_t(x, t) = -q_1 \tilde{\alpha}_x(x, t) - c_1 \tilde{\alpha}(x, t) \quad (23)$$

$$\tilde{\beta}_t(x, t) = q_2 \tilde{\beta}_x(x, t) - c_2 \tilde{\beta}(x, t) \quad (24)$$

$$\tilde{\beta}(1, t) = q \tilde{\alpha}(1, t) + C \tilde{Z}(t) + (\bar{\varphi}(1) - q \bar{\gamma}(1)) \tilde{Y}(t) \quad (25)$$

$$\begin{pmatrix} \dot{\tilde{Y}}(t) \\ \dot{\tilde{Z}}(t) \end{pmatrix} = \begin{pmatrix} \bar{A}_0 & 0 \\ I_a & \bar{A} \end{pmatrix} \begin{pmatrix} \tilde{Y}(t) \\ \tilde{Z}(t) \end{pmatrix} - \begin{pmatrix} \Psi_0 \\ 0 \end{pmatrix} \tilde{\beta}(0, t) \quad (26)$$

where  $I_a = \Psi_3 \bar{\varphi}(0) - B \bar{\gamma}(1) - L(\bar{\varphi}(1) - q \bar{\gamma}(1))$ , and where the in-domain couplings of the transport PDEs are removed and the system matrix in (26) is Hurwitz because the matrices  $\bar{A}$  and  $\bar{A}_0$  are Hurwitz defined in (8) and (10). The target observer error system (22)–(26) has an analogous structure with (57), (59) in [16]. The observer gains  $\Psi_0, \Psi_1(x), \Psi_2(x), \Psi_3$  are obtained

as

$$\Psi_1(x) = -q_2\bar{\phi}_1(x, 0) - \bar{\gamma}(x)L_0 \quad (27)$$

$$\Psi_2(x) = -q_2\bar{\psi}_1(x, 0) - \bar{\phi}(x)L_0 \quad (28)$$

$$\Psi_0 = L_0, \quad \Psi_3 = \bar{K}_2(0)q_2. \quad (29)$$

*Lemma 1:* Consider the observer (12)–(17) with the observer gains (27)–(29) applied to the system (1)–(6). The resulting observer error system- $(\tilde{z}(x, t), \tilde{w}(x, t), \tilde{X}(t), \tilde{Y}(t))$ , for all initial data  $(\tilde{z}(x, 0), \tilde{w}(x, 0), \tilde{X}(0), \tilde{Y}(0)) \in L^2(0, 1) \times L^2(0, 1) \times \mathbb{R}^n \times \mathbb{R}^{\bar{n}}$ , is exponentially stable in the sense that there exist positive constants  $\Upsilon_e, \lambda_e$  such that

$$\begin{aligned} & \left| \tilde{X}(t) \right|^2 + \left| \tilde{Y}(t) \right|^2 + \|\tilde{z}(\cdot, t)\|^2 + \|\tilde{w}(\cdot, t)\|^2 \\ & \leq \Upsilon_e \left( \left| \tilde{X}(0) \right|^2 + \left| \tilde{Y}(0) \right|^2 + \|\tilde{z}(\cdot, 0)\|^2 + \|\tilde{w}(\cdot, 0)\|^2 \right) e^{-\lambda_e t} \end{aligned} \quad (30)$$

where the decay rate  $\lambda_e$  depends on the choices of  $L, L_0$  in (8) and (10).

*Proof:* Through a traditional Lyapunov analysis for the target observer error system (22)–(26), the exponential stability is obtained, whose exponential convergence rate is determined by the eigenvalue assignment for  $\bar{A} = A - LC$  and  $\bar{A}_0 = A_0 - L_0 C_0$ , i.e., the choices of  $L, L_0$ . Applying the invertibility of the backstepping transformations (19), (20), and (21), this lemma is obtained. ■

#### IV. CONTINUOUS-IN-TIME CONTROL LAW

Before designing the event-triggered controller  $U_d(t)$ , a continuous-in-time feedback controller  $U(t)$  is developed to exponentially stabilize the sandwich plant in this section. The proximal reflection term is compensated by the control input going through the ODE at the input channel. As a result the continuous-in-time control law includes  $n_r$ -order time derivatives of  $w(0, t)$  where  $n_r$  is the relative degree of the ODE. This high-order term would cause difficulties in designing the subsequent event-triggering mechanism guaranteeing the existence of a minimal dwell-time between two triggering times. A low-pass-filter-based modification of the backstepping control design is presented to address this problem.

The continuous-in-time control is derived by conducting a state-feedback design based on the observer (12)–(17) with output estimation error injection terms assumed absent, in accordance to the result on their asymptotic convergence to zero in Lemma 1 (complete (12)–(17) is only used in the simulation). The separation principle is then verified and applied in the stability analysis of the resulting closed-loop system.

##### A. First Transformation

In order to remove the in-domain couplings between the PDEs and make the system matrix of the ODE at the right boundary Hurwitz, we introduce a PDE backstepping transformation

$$\begin{aligned} \alpha(x, t) &= \tilde{z}(x, t) - \int_x^1 M(x, y)\tilde{z}(y, t)dy \\ &\quad - \int_x^1 N(x, y)\hat{w}(y, t)dy - \gamma(x)\hat{X}(t) \end{aligned} \quad (31)$$

$$\begin{aligned} \beta(x, t) &= \hat{w}(x, t) - \int_x^1 H(x, y)\hat{z}(y, t)dy \\ &\quad - \int_x^1 J(x, y)\hat{w}(y, t)dy - \lambda(x)\hat{X}(t) \end{aligned} \quad (32)$$

with  $M(x, y), N(x, y), \gamma(x), H(x, y), J(x, y), \lambda(x)$  satisfying conditions (B.1)–(B.12) in the Appendix, whose well-posedness is proved in [43, Lemma 1]. With this transformation, the system (12)–(17) with the observer errors assumed absent, is converted to

$$\begin{aligned} \dot{\hat{Y}}(t) &= A_0\hat{Y}(t) + E_0 \left( \beta(0, t) - \int_0^1 \bar{K}_4(0, y)\alpha(y, t)dy \right. \\ &\quad \left. - \int_0^1 \bar{K}_5(0, y)\beta(y, t)dy - \bar{K}_6\hat{X}(t) \right) + B_0U(t) \end{aligned} \quad (33)$$

$$\begin{aligned} \alpha(0, t) &= p\beta(0, t) + \int_0^1 \bar{K}_1(x)\alpha(x, t)dx + C_0\hat{Y}(t) \\ &\quad + \int_0^1 \bar{K}_2(x)\beta(x, t)dx + \bar{K}_3\hat{X}(t) \end{aligned} \quad (34)$$

$$\alpha_t(x, t) = -q_1\alpha_x(x, t) - c_1\alpha(x, t) \quad (35)$$

$$\beta_t(x, t) = q_2\beta_x(x, t) - c_2\beta(x, t) \quad (36)$$

$$\beta(1, t) = q\alpha(1, t) \quad (37)$$

$$\dot{\hat{X}}(t) = \hat{A}\hat{X}(t) + B\alpha(1, t) \quad (38)$$

where  $\hat{A} = A - BK$  is Hurwitz in light of Assumption 1, and the gains  $\bar{K}_1(x), \bar{K}_2(x), \bar{K}_3, \bar{K}_4(x), \bar{K}_5(x), \bar{K}_6$  are shown in (C.1)–(C.6) in the Appendix.

##### B. Second Transformation

Similar to [49], a transformation is used to remove the additional terms introduced by the transformation (31), (32) at the left boundary, so that they can be compensated by the design of the control input. This transformation is given by

$$\begin{aligned} \hat{Z}(t) &= \hat{Y}(t) + C_0^+ \int_0^1 \bar{K}_1(x)\alpha(x, t)dx \\ &\quad + C_0^+ \int_0^1 \bar{K}_2(x)\beta(x, t)dx + C_0^+ \bar{K}_3\hat{X}(t) \end{aligned} \quad (39)$$

where  $C_0^+$  is a right inverse matrix of  $C_0$ . Because  $C_0$  is full-row rank according to Assumption 2, a right inverse exists for  $C_0$ .

Then, (33), (34) are converted to

$$\begin{aligned} \dot{\hat{Z}}(t) &= \hat{A}_0\hat{Z}(t) + q_1C_0^+\bar{K}_1(0)C_0\hat{Z}(t) + B_0\bar{U}(t) \\ &\quad + M_X\hat{X}(t) + \int_0^1 M_\alpha(x)\alpha(x, t)dx \\ &\quad + \int_0^1 M_\beta(x)\beta(x, t)dx + N_1\alpha(1, t) + N_2\beta(0, t) \end{aligned} \quad (40)$$

$$\alpha(0, t) = p\beta(0, t) + C_0\hat{Z}(t) \quad (41)$$

where

$$\bar{U}(t) = U(t) - K_0\hat{Z}(t) \quad (42)$$

and  $K_0$  is chosen to make  $\hat{A}_0$  Hurwitz according to Assumption 1. The scalars  $N_1, N_2, M_\alpha, M_\beta, M_X$  are shown in (D.1)–(D.5) in the Appendix.

### C. Third Transformation With Frequency Domain Design

Taking the Laplace transformation of (35)–(38), (40), (41), we have

$$\begin{aligned} (sI - \hat{A}_0)\hat{Z}(s) &= q_1 C_0^+ \bar{K}_1(0) C_0 \hat{Z}(s) + M_X \hat{X}(s) \\ &+ \int_0^1 M_\alpha(x) \alpha(x, s) dx + \int_0^1 M_\beta(x) \beta(x, s) dx \\ &+ N_1 \alpha(1, s) + N_2 \beta(0, s) + B_0 \bar{U}(s) \quad (43) \\ \alpha(0, s) &= p \beta(0, s) + C_0 \hat{Z}(s) \quad (44) \\ s \alpha(x, s) &= -q_1 \alpha_x(x, s) - c_1 \alpha(x, s) \quad (45) \\ s \beta(x, s) &= q_2 \beta_x(x, s) - c_2 \beta(x, s) \quad (46) \\ \beta(1, s) &= q \alpha(1, s) \quad (47) \\ (sI - \hat{A})\hat{X}(s) &= B \alpha(1, s). \quad (48) \end{aligned}$$

For brevity, we consider all the initial conditions to be zero while taking the Laplace transform (arbitrary initial conditions could be incorporated into the stability statement through a routine expanded analysis).

Recalling that  $\hat{A}_0$  is Hurwitz,  $\det(sI - \hat{A}_0)$  does not have any zeros in the closed right-half plane. Multiplying both sides of (43) with  $(sI - \hat{A}_0)^{-1}$ , we get

$$\begin{aligned} \hat{Z}(s) &= (sI - \hat{A}_0)^{-1} \left[ q_1 C_0^+ \bar{K}_1(0) C_0 \hat{Z}(s) + M_X \hat{X}(s) \right. \\ &+ \int_0^1 M_\alpha(x) \alpha(x, s) dx + \int_0^1 M_\beta(x) \beta(x, s) dx \\ &\left. + N_1 \alpha(1, s) + N_2 \beta(0, s) + B_0 \bar{U}(s) \right]. \quad (49) \end{aligned}$$

In order to cancel the proximal reflection term  $\beta(0, s)$  in (44), the following transformation:

$$\hat{W}(s) = C_0^+ p \beta(0, s) + \hat{Z}(s) \quad (50)$$

is applied to (49) and (44), yielding

$$\begin{aligned} \hat{W}(s) &= (sI - \hat{A}_0)^{-1} \left[ q_1 C_0^+ \bar{K}_1(0) C_0 \hat{W}(s) + M_X \hat{X}(s) \right. \\ &+ \int_0^1 M_\alpha(x) \alpha(x, s) dx + \int_0^1 M_\beta(x) \beta(x, s) dx \\ &\left. + N_1 \alpha(1, s) + \bar{N}_2 \beta(0, s) \right] + (sI - \hat{A}_0)^{-1} B_0 \bar{U}(s) \\ &+ C_0^+ p \beta(0, s) \quad (51) \end{aligned}$$

$$\alpha(0, s) = C_0 \hat{W}(s) \quad (52)$$

where  $\bar{N}_2 = N_2 - q_1 C_0^+ \bar{K}_1(0) p$ . Together with (45)–(48), we have the following relationships:

$$\alpha(x, s) = e^{\left(\frac{c_1-s}{q_1}\right)x} C_0 \hat{W}(s) \quad (53)$$

$$\beta(x, s) = q e^{\left(\frac{c_2-s}{q_2}\right)(1-x) + \left(\frac{c_1-s}{q_1}\right)} C_0 \hat{W}(s) \quad (54)$$

$$\alpha(0, s) = C_0 \hat{W}(s) \quad (55)$$

$$\beta(1, s) = q e^{\left(\frac{c_1-s}{q_1}\right)} C_0 \hat{W}(s) \quad (56)$$

$$\beta(0, s) = q e^{\left(\frac{c_2-s}{q_2}\right) + \left(\frac{c_1-s}{q_1}\right)} C_0 \hat{W}(s) \quad (57)$$

$$\alpha(1, s) = e^{\left(\frac{c_1-s}{q_1}\right)} C_0 \hat{W}(s) \quad (58)$$

$$\hat{X}(s) = (sI - \hat{A})^{-1} B e^{\left(\frac{c_1-s}{q_1}\right)} C_0 \hat{W}(s) \quad (59)$$

$$\begin{aligned} \int_0^1 M_\beta(y) \beta(y, s) dy \\ = \int_0^1 M_\beta(y) q e^{\left(\frac{c_2-s}{q_2}\right)(1-y) + \left(\frac{c_1-s}{q_1}\right)} dy C_0 \hat{W}(s) \quad (60) \end{aligned}$$

$$\int_0^1 M_\alpha(y) \alpha(y, s) dy = \int_0^1 M_\alpha(y) e^{\left(\frac{c_1-s}{q_1}\right)y} dy C_0 \hat{W}(s). \quad (61)$$

Inserting (53)–(61) into (51), and multiplying by  $C_0$  on both sides, we have

$$\begin{aligned} C_0 \hat{W}(s) &= C_0 (sI - \hat{A}_0)^{-1} \left[ q_1 C_0^+ \bar{K}_1(0) C_0 \hat{W}(s) \right. \\ &+ M_X (sI - \hat{A})^{-1} B e^{\left(\frac{c_1-s}{q_1}\right)} C_0 \hat{W}(s) \\ &+ \int_0^1 M_\alpha(y) e^{\left(\frac{c_1-s}{q_1}\right)y} dy C_0 \hat{W}(s) \\ &+ \int_0^1 M_\beta(y) q e^{\left(\frac{c_2-s}{q_2}\right)(1-y) + \left(\frac{c_1-s}{q_1}\right)} dy C_0 \hat{W}(s) \\ &+ N_1 e^{\left(\frac{c_1-s}{q_1}\right)} C_0 \hat{W}(s) + \bar{N}_2 q e^{\left(\frac{c_2-s}{q_2}\right) + \left(\frac{c_1-s}{q_1}\right)} C_0 \hat{W}(s) \\ &\left. + C_0 (sI - \hat{A}_0)^{-1} B_0 \bar{U}(s) + p q e^{\left(\frac{c_2-s}{q_2}\right) + \left(\frac{c_1-s}{q_1}\right)} C_0 \hat{W}(s) \right]. \quad (62) \end{aligned}$$

We use the definition of a (strictly) proper transfer function for infinite-dimensional systems from [10].

**Definition 1:** A transfer function  $G$  is said to be proper if for, sufficiently large  $h$ ,  $\sup_{\text{Re}(s) \geq 0} \cap_{|s| > h} |G(s)| < \infty$ . If the limit of  $G(s)$  at infinity exists and is 0, we say that  $G$  is strictly proper.

According to [10], the definition of an asymptotically stable transfer function for infinite-dimensional systems is given next.

**Definition 2:** A transfer function  $G(s)$  is said to be asymptotically stable if it satisfies  $\sup_{\text{Re}(s) \geq 0} |G(s)| < \infty$ .

Definition 2 indicates there is no pole in the closed right-half plane. For the sake of brevity of exposition, when we refer to a transfer function as stable, we mean asymptotically stable.

Define a new variable as

$$\xi(s) = C_0 \hat{W}(s). \quad (63)$$

Equation (62) is, thus, rewritten as

$$\begin{aligned} \xi(s) &= \left[ C_0 (sI - \hat{A}_0)^{-1} G(s) + p q e^{\left(\frac{c_2-s}{q_2} + \frac{c_1-s}{q_1}\right)} \right] \xi(s) \\ &+ C_0 (sI - \hat{A}_0)^{-1} B_0 \bar{U}(s) \quad (64) \end{aligned}$$

where

$$G(s) = q_1 C_0^+ \bar{K}_1(0) + M_X (sI - \hat{A})^{-1} B e^{\left(\frac{c_1-s}{q_1}\right)}$$

$$\begin{aligned}
& + \int_0^1 M_\alpha(y) e^{\left(\frac{c_1-s}{q_1}\right)y} dy \\
& + \int_0^1 M_\beta(y) q e^{\left(\frac{c_2-s}{q_2}\right)(1-y) + \left(\frac{c_1-s}{q_1}\right)} dy \\
& + N_1 e^{\left(\frac{c_1-s}{q_1}\right)} + \bar{N}_2 q e^{\left(\frac{c_2-s}{q_2} + \frac{c_1-s}{q_1}\right)} \tag{65}
\end{aligned}$$

is a vector of stable, proper transfer functions because there is no pole in the closed right half-plane (since  $\hat{A}$  is Hurwitz). The definitions of proper, stable properties of irrational transfer functions are given in Definitions 1 and 2.

Using Assumption 2, according to [34], we get

$$C_0(sI - \hat{A}_0)^{-1} B_0 \neq 0.$$

We now choose  $\bar{U}(s)$  in (64) as

$$\bar{U}(s) = -F(s)\xi(s) \tag{66}$$

where

$$\begin{aligned}
F(s) = & \frac{\Omega(s)}{C_0(sI - \hat{A}_0)^{-1} B_0} \left[ C_0(sI - \hat{A}_0)^{-1} G(s) \right. \\
& \left. + p q e^{\left(\frac{c_2-s}{q_2}\right) + \left(\frac{c_1-s}{q_1}\right)} \right]. \tag{67}
\end{aligned}$$

The transfer function  $\Omega(s)$  is a stable SISO low-pass filter of sufficient order to be designed, which makes  $F(s)$  (strictly) proper and satisfies

$$|\Phi(s)| < 1 \tag{68}$$

for all  $s \in \mathbb{C}$ ,  $\Re(s) \geq 0$ , where

$$\Phi(s) = (1 - \Omega(s)) \left( C_0(sI - \hat{A}_0)^{-1} G(s) + p q e^{\left(\frac{c_2-s}{q_2}\right) + \left(\frac{c_1-s}{q_1}\right)} \right). \tag{69}$$

The matrix  $\hat{A}_0$  being Hurwitz and  $G(s)$  in (65) being a stable, proper transfer matrix, along with Assumption 3, ensures the existence of the low-pass filter  $\Omega(s)$  satisfying (68) when  $s$  approaches infinity along the imaginary axis, so a low-pass filter  $\Omega(s)$  exists with the desired properties for all  $s \in \mathbb{C}$ ,  $\Re(s) \geq 0$ . The transfer function  $F(s)$  (67) is stable and proper because there is no pole in the closed right half-plane.

According to (32), (57), (63), (66), and (67), the control design contains the signal  $\frac{\beta(0,s)}{C_0(sI - \hat{A}_0)^{-1} B_0}$ , which is associated with  $n_r$ -order time derivatives of  $\hat{W}(0, t)$  (the initial condition is, thus, set in  $\chi$  defined below (1)–(6)) and enters into the low-pass filter  $\Omega(s)$ .

Inserting  $\bar{U}(s)$  defined by (66), then (64) becomes

$$(1 - \Phi(s))\xi(s) = 0 \tag{70}$$

where  $\Phi(s)$  is given in (69) and satisfies (68).

In the continuous-in-time control design in this section, (68) and (70) ensure the exponential convergence to zero of  $\xi$ . The exponential convergence to zero of  $\hat{W}$  is obtained by recalling (51), with (53)–(61), (63), and (66) incorporated (the resulting transfer functions before  $\xi(s)$  on the right-hand side of the resulting equation, whose left-hand side is  $\hat{W}(s)$ , are proper and stable). The exponential convergence to zero of the signals in the  $\alpha, \beta$  PDEs and the distal  $\hat{X}$  ODE are also obtained by recalling the relationships (53)–(61).

Recalling (42), (66), the continuous-in-time control law, in  $s$  domain, is obtained as

$$U(s) = K_0 \hat{Z}(s) + \bar{U}(s) = K_0 \hat{Z}(s) - F(s)\xi(s) \tag{71}$$

based on which the event-triggering mechanism is designed in the following section.

## V. EVENT-TRIGGERING MECHANISM

In this section, we introduce an event-triggered control scheme for stabilization of the  $2 \times 2$  hyperbolic PDE sandwiched system (1)–(6). This scheme relies on both the continuous-in-time control  $U(t)$ , designed in the last section, and a dynamic event-triggering mechanism (ETM), which determines triggering times. The event-triggered control signal  $U_d(t)$  is the value of the continuous-in-time  $U(t)$  at the time instants  $t_k$  but applied until time  $t_{k+1}$ , i.e.,

$$U_d(t) = U(t_k), \quad t \in [t_k, t_{k+1}). \tag{72}$$

A deviation  $d(t)$  between the continuous-in-time control signal and the event-based one is given as

$$d(t) = U(t) - U_d(t). \tag{73}$$

Recalling (71), we know that

$$U_d(s) = U(s) - d(s) = K_0 \hat{Z}(s) - F(s)\xi(s) - d(s). \tag{74}$$

Replacing  $U(s)$  by  $U_d(s)$  in the control design in the last section, applying (74), the relation (70) becomes

$$(1 - \Phi(s))\xi(s) = C_0(sI - \hat{A}_0)^{-1} B_0 d(s). \tag{75}$$

Multiplying both sides of (51) (where  $\bar{U}(s) = -F(s)\xi(s) - d(s)$  now) with  $(sI - \hat{A}_0)$ , and inserting (53)–(61), (66), (75), yields

$$s\hat{W}(s) = \hat{A}_0 \hat{W}(s) + D(s)d(s) \tag{76}$$

where

$$\begin{aligned}
D(s) = & \left( G(s) - B_0 F(s) + (sI - \hat{A}_0) C_0^+ p q e^{\left(\frac{c_2-s}{q_2}\right) + \left(\frac{c_1-s}{q_1}\right)} \right) \\
& \times \frac{C_0(sI - \hat{A}_0)^{-1} B_0}{1 - \Phi(s)} - B_0 \tag{77}
\end{aligned}$$

is an  $\bar{n}$ -dimensional column vector of stable, proper transfer functions. The components of  $D(s)$  are stable, i.e., they have no right half-plane poles, due to (65), (67),  $\hat{A}_0$  being Hurwitz, and  $1 - \Phi(s) \neq 0$  for all  $s \in \mathbb{C}$ ,  $\Re(s) \geq 0$ . Let us denote

$$\mathcal{D}(d(t))_{\bar{n} \times 1} = \mathcal{L}^{-1}(D(s)d(s))$$

which is the inverse Laplace transformation of  $D(s)d(s)$ , i.e., of the outputs of the system  $D(s)$  under the input  $d(s)$ . The stable, proper  $D(s)$  guarantees a Bounded-Input Bounded-Output (BIBO) relationship, so that the following estimate holds:

$$\mathcal{D}(d(t))^2 \leq \bar{d} \sup_{0 \leq \zeta \leq t} d(\zeta)^2 \tag{78}$$

where the constant  $\bar{d} > 0$  is associated with the  $L_1$  norm of the impulse responses ([13, CH.2], [29, Appendix B]) of the entries of  $D(s)$  in (77). It follows that  $\bar{d}$  only depends on the parameters of the plant and of the low-pass-filter-based backstepping continuous-in-time control law.

Recalling (35)–(38), (52), and (76), the event-based target system in the time domain is obtained as

$$\dot{\hat{W}}(t) = \hat{A}_0 \hat{W}(t) + \mathcal{D}(d(t)) \tag{79}$$

$$\alpha(0, t) = C_0 \hat{W}(t) \quad (80)$$

$$\alpha_t(x, t) = -q_1 \alpha_x(x, t) - c_1 \alpha(x, t) \quad (81)$$

$$\beta_t(x, t) = q_2 \beta_x(x, t) - c_2 \beta(x, t) \quad (82)$$

$$\beta(1, t) = q\alpha(1, t) \quad (83)$$

$$\dot{\hat{X}}(t) = \hat{A}\hat{X}(t) + B\alpha(1, t). \quad (84)$$

The ETM to determine the triggering times is designed to be governed by the following dynamic triggering condition [20]:

$$t_{k+1} = \inf\{t \in R^+ | t > t_k | d(t)^2 \geq \theta \hat{W}^T(t) P_0 \hat{W}(t) - \mu m(t)\} \quad (85)$$

where the internal dynamic variable  $m(t)$  satisfies the ordinary differential equation

$$\dot{m}(t) = -\eta m(t) - \mu_W \sup_{0 \leq \zeta \leq t} |\hat{W}(\zeta)|^2 - \mu_d \sup_{0 \leq \zeta \leq t} d(\zeta)^2 \quad (86)$$

with initial condition  $m(0) < 0$ , which guarantees that

$$m(t) < 0. \quad (87)$$

Inequality (87) follows from the ODE (86), the nonpositivity of the nonhomogeneous terms on its right-hand side, the strict negativity of  $m(0)$ , the variation-of-constants formula, and the comparison principle. Thus, the fact that  $m(t) < 0$  would not be affected by (85).

The positive definite matrix  $P_0 = P_0^T$  in (85) is the unique solution to the Lyapunov equation

$$\hat{A}_0^T P_0 + P_0 \hat{A}_0 = -Q_0 \quad (88)$$

for some  $Q_0 = Q_0^T > 0$ . The positive constants  $\theta, \mu, \eta, \mu_W, \mu_d$  in ETM are to be determined later.

The observer-based event-triggering condition (85) uses the transformed ODE state  $\hat{W}(t)$  because it contains the estimated states of the overall ODE-PDE-ODE system through the transformations (31), (32), (39), (50).

As will be seen in Lemma 2,  $\dot{d}(t)^2$ , on which the minimal dwell-time relies, is bounded by  $\sup_{0 \leq \zeta \leq t} |\hat{W}(\zeta)|^2$ ,  $\sup_{0 \leq \zeta \leq t} d(\zeta)^2$  (instead of  $|\hat{W}(t)|^2, d(t)^2$  in (85)), in order to avoid the Zeno phenomenon, namely, to ensure that  $\lim_{k \rightarrow +\infty} t_k = +\infty$ , the internal dynamic variable  $m(t)$  is introduced in (85) to offset  $\sup_{0 \leq \zeta \leq t} |\hat{W}(\zeta)|^2, \sup_{0 \leq \zeta \leq t} d(\zeta)^2$  when proving the existence of a minimal dwell-time, which will be seen clearly in the proof of Lemma 3.

**Proposition 1:** For given  $(z(\cdot, t_k), w(\cdot, t_k))^T \in L^2((0, 1); \mathbb{R}^2)$ ,  $X(t_k) \in \mathbb{R}^n$ ,  $Y(t_k) \in \mathbb{R}^{\bar{n}}$  and  $(\hat{z}(\cdot, t_k), \hat{w}(\cdot, t_k))^T \in L^2((0, 1); \mathbb{R}^2)$ ,  $\hat{X}(t_k) \in \mathbb{R}^n$ ,  $\hat{Y}(t_k) \in \mathbb{R}^{\bar{n}}$ ,  $m(t_k) \in \mathbb{R}^-$ , there exist unique (weak) solutions  $((z, w)^T, X, Y) \in C^0([t_k, t_{k+1}]; L^2(0, 1); \mathbb{R}^2) \times C^0([t_k, t_{k+1}]; \mathbb{R}^n) \times C^0([t_k, t_{k+1}]; \mathbb{R}^{\bar{n}})$  and  $((\hat{z}, \hat{w})^T, \hat{X}, \hat{Y}) \in C^0([t_k, t_{k+1}]; L^2(0, 1); \mathbb{R}^2) \times C^0([t_k, t_{k+1}]; \mathbb{R}^n) \times C^0([t_k, t_{k+1}]; \mathbb{R}^{\bar{n}})$ ,  $m \in C^0([t_k, t_{k+1}]; \mathbb{R}^-)$  to the systems (1)–(6) and (12)–(17), (86) with the event-based control input  $U_d(t)$  applied in (1) and (12), respectively, between two time instants  $t_k$  and  $t_{k+1}$ .

**Proof:** For given  $(\tilde{z}(\cdot, t_k), \tilde{w}(\cdot, t_k))^T \in L^2((0, 1); \mathbb{R}^2)$ ,  $\tilde{X}(t_k) \in \mathbb{R}^n$  and  $\tilde{Y}(t_k) \in \mathbb{R}^{\bar{n}}$ , it can be shown that there exists a unique solution  $((\tilde{z}, \tilde{w})^T, \tilde{X}, \tilde{Y}) \in C^0([t_k, t_{k+1}]; L^2(0, 1); \mathbb{R}^2) \times C^0([t_k, t_{k+1}]; \mathbb{R}^n) \times C^0([t_k, t_{k+1}]; \mathbb{R}^{\bar{n}})$  of the

observer error system by recalling the target observer error system (22)–(26), which is well-known to be well-posed for a given initial data, as well as the backstepping transformations (19), (20), and (21). Adopting the notion of the weak solution given in the book [7] (Definition A.5), for given  $(z(\cdot, t_k), w(\cdot, t_k))^T \in L^2((0, 1); \mathbb{R}^2)$ ,  $X(t_k) \in \mathbb{R}^n$  and  $Y(t_k) \in \mathbb{R}^{\bar{n}}$ , with the results in [12], [38], it can be shown that there exists a unique (weak) solution  $((z, w)^T, X, Y) \in C^0([t_k, t_{k+1}]; L^2(0, 1); \mathbb{R}^2) \times C^0([t_k, t_{k+1}]; \mathbb{R}^n) \times C^0([t_k, t_{k+1}]; \mathbb{R}^{\bar{n}})$  to the system (1)–(6) under the event-based control input  $U_d(t)$ . Recalling (18), it can then be shown that there exists a unique (weak) solution  $((\hat{z}, \hat{w})^T, \hat{X}, \hat{Y}) \in C^0([t_k, t_{k+1}]; L^2(0, 1); \mathbb{R}^2) \times C^0([t_k, t_{k+1}]; \mathbb{R}^n) \times C^0([t_k, t_{k+1}]; \mathbb{R}^{\bar{n}})$  and  $m \in C^0([t_k, t_{k+1}]; \mathbb{R}^-)$  to the system (12)–(17), (86) under the event-based control input  $U_d(t)$ . Proposition 1 is, thus, obtained. ■

**Lemma 2:** Considering  $d(t)$  defined in (73), there exist positive constants  $\lambda_W, \lambda_d$  such that

$$\dot{d}(t)^2 \leq \lambda_W \sup_{0 \leq \zeta \leq t} |\hat{W}(\zeta)|^2 + \lambda_d \sup_{0 \leq \zeta \leq t} d(\zeta)^2 \quad (89)$$

for  $t \in (t_k, t_{k+1})$ , where  $\lambda_W, \lambda_d$  only depend on parameters of the plant and the low-pass-filter-based backstepping continuous-in-time control law.

**Proof:** Taking the time derivative of (73), we have

$$\dot{d}(t)^2 = \dot{U}(t)^2 \quad (90)$$

because of  $\dot{U}_d(t) = 0$  for  $t \in (t_k, t_{k+1})$ . Recalling (50), (57), (71), (76), we get

$$sU(s) = R(s)\hat{W}(s) + R_d(s)d(s) \quad (91)$$

where

$$R(s) = \left( K_0 - \left( K_0 C_0^+ p q e^{\left( \frac{c_2-s}{q_2} \right) + \left( \frac{c_1-s}{q_1} \right)} + F(s) \right) C_0 \right) \hat{A}_0 \quad (92)$$

is an  $\bar{n}$ -dimensional row vector of stable, proper transfer functions, and

$$R_d(s) = \left( K_0 - \left( K_0 C_0^+ p q e^{\left( \frac{c_2-s}{q_2} \right) + \left( \frac{c_1-s}{q_1} \right)} + F(s) \right) C_0 \right) D(s) \quad (93)$$

is a stable, proper transfer function ( $F(s)$  and  $D(s)$  are stable and proper). We, thus, have BIBO with the estimate

$$\dot{U}(t)^2 \leq \lambda_W \sup_{0 \leq \zeta \leq t} |\hat{W}(\zeta)|^2 + \lambda_d \sup_{0 \leq \zeta \leq t} d(\zeta)^2 \quad (94)$$

where  $\lambda_W$  is associated with the  $\|\cdot\|_1$  norm of the impulse responses of the entries of the transfer function vector  $R(s)$ , and  $\lambda_d$  is, likewise, associated with  $\|R_d\|_1$ , which only depend on the plant and the design of the continuous-in-time control law. ■

The following lemma proves the existence of a minimal dwell-time between two triggering times (independent of initial conditions). It ensures that the Zeno phenomenon does not occur and the achievement of a reduction of changes in the value in the actuator signal compared with the continuous-in-time control.

**Lemma 3:** For some  $\mu_W, \mu_d, \theta$ , there exists a minimal dwell-time  $\tau > 0$ , independent of initial conditions, between any two successive triggering times, i.e.,  $t_{k+1} - t_k \geq \tau$  for all  $k \geq 0$ .

*Proof:* Let us introduce the function

$$\psi(t) = \frac{d(t)^2 + \frac{\mu}{2}m(t)}{\theta\hat{W}^T(t)P_0\hat{W}(t) - \frac{\mu}{2}m(t)} \quad (95)$$

which was proposed in [20]. We have that  $\psi(t_{k+1}) = 1$  because the event is triggered, and  $\psi(t_k) < 0$  because of  $m(t) < 0$  and  $d(t_k) = 0$ . The function  $\psi(t)$  is continuous on  $[t_k, t_{k+1}]$  due to Proposition 1. By the intermediate value theorem, there exists  $t^* > t_k$  such that  $\psi(t) \in [0, 1]$  when  $t \in [t^*, t_{k+1}]$ . The minimal  $\tau$  can be defined as the minimal time it takes for  $\psi(t)$  from 0 to 1, i.e., the reciprocal of the absolute value of the maximum  $\dot{\psi}(t)$ .

Recalling (78), (79), we have that

$$\begin{aligned} \frac{\hat{W}^T(t)P_0\hat{W}(t)}{dt} &\geq -\frac{3}{2}\lambda_{\max}(Q_0) \left| \hat{W}(t) \right|^2 \\ &\quad - \frac{2\bar{\lambda}_{\max}(P_0)^2}{\lambda_{\max}(Q_0)} \sup_{0 \leq \zeta \leq t} d(\zeta)^2. \end{aligned} \quad (96)$$

Taking the derivative of  $\psi(t)$  (95) and using (89), (96), we have

$$\begin{aligned} \dot{\psi}(t) &= \frac{2d(t)\dot{d}(t) + \frac{\mu}{2}\dot{m}(t)}{\theta\hat{W}^T(t)P_0\hat{W}(t) - \frac{\mu}{2}m(t)} \\ &\quad - \frac{\theta\frac{\dot{W}^T(t)P_0\hat{W}(t)}{dt} - \frac{\mu}{2}\dot{m}(t)}{\theta\hat{W}^T(t)P_0\hat{W}(t) - \frac{\mu}{2}m(t)}\psi(t) \\ &\leq \frac{1}{\theta\hat{W}^T(t)P_0\hat{W}(t) - \frac{\mu}{2}m(t)} \times \left[ r_1\lambda_W \sup_{0 \leq \zeta \leq t} \left| \hat{W}(\zeta) \right|^2 \right. \\ &\quad \left. + r_1\lambda_d \sup_{0 \leq \zeta \leq t} d(\zeta)^2 + \frac{1}{r_1}d(t)^2 + \frac{\mu}{2}\dot{m}(t) \right] \\ &\quad - \frac{1}{\theta\hat{W}^T(t)P_0\hat{W}(t) - \frac{\mu}{2}m(t)} \\ &\quad \times \left[ \theta \left( -\frac{3}{2}\lambda_{\max}(Q_0) \left| \hat{W}(t) \right|^2 \right. \right. \\ &\quad \left. \left. - \frac{2\bar{\lambda}_{\max}(P_0)^2}{\lambda_{\max}(Q_0)} \sup_{0 \leq \zeta \leq t} d(\zeta)^2 \right) - \frac{\mu}{2}\dot{m}(t) \right] \psi(t) \end{aligned} \quad (97)$$

where  $r_1$  is a positive constant from Young's inequality. Inserting (86), one obtains

$$\begin{aligned} \dot{\psi}(t) &\leq \frac{1}{\theta\hat{W}^T(t)P_0\hat{W}(t) - \frac{\mu}{2}m(t)} \left[ r_1\lambda_W \sup_{0 \leq \zeta \leq t} \left| \hat{W}(\zeta) \right|^2 \right. \\ &\quad \left. + r_1\lambda_d \sup_{0 \leq \zeta \leq t} d(\zeta)^2 + \frac{1}{r_1}d(t)^2 - \frac{\mu}{2}\eta m(t) \right. \\ &\quad \left. - \frac{\mu}{2}\mu_W \sup_{0 \leq \zeta \leq t} \left| \hat{W}(\zeta) \right|^2 - \frac{\mu}{2}\mu_d \sup_{0 \leq \zeta \leq t} d(\zeta)^2 \right] \\ &\quad - \frac{1}{\theta\hat{W}^T(t)P_0\hat{W}(t) - \frac{\mu}{2}m(t)} \\ &\quad \times \left[ -\frac{3\theta}{2}\lambda_{\max}(Q_0) \left| \hat{W}(t) \right|^2 \right. \\ &\quad \left. - \frac{2\theta\bar{\lambda}_{\max}(P_0)^2}{\lambda_{\max}(Q_0)} \sup_{0 \leq \zeta \leq t} d(\zeta)^2 + \frac{\mu}{2}\eta m(t) \right] \end{aligned}$$

$$\begin{aligned} &\quad + \frac{\mu}{2}\mu_W \sup_{0 \leq \zeta \leq t} \left| \hat{W}(\zeta) \right|^2 + \frac{\mu}{2}\mu_d \sup_{0 \leq \zeta \leq t} d(\zeta)^2 \Big] \psi(t) \\ &\leq \frac{1}{\theta\hat{W}^T(t)P_0\hat{W}(t) - \frac{\mu}{2}m(t)} \\ &\quad \times \left[ \left( r_1\lambda_W - \frac{\mu}{2}\mu_W \right) \sup_{0 \leq \zeta \leq t} \left| \hat{W}(\zeta) \right|^2 \right. \\ &\quad \left. + \left( r_1\lambda_d - \frac{\mu}{2}\mu_d \right) \sup_{0 \leq \zeta \leq t} d(\zeta)^2 + \frac{1}{r_1}d(t)^2 - \frac{\mu}{2}\eta m(t) \right] \\ &\quad + \frac{1}{\theta\hat{W}^T(t)P_0\hat{W}(t) - \frac{\mu}{2}m(t)} \left[ -\frac{\mu}{2}\eta m(t) \right. \\ &\quad \left. + \left( \frac{3\theta}{2}\lambda_{\max}(Q_0) - \frac{\mu}{2}\mu_W \right) \sup_{0 \leq \zeta \leq t} \left| \hat{W}(\zeta) \right|^2 \right. \\ &\quad \left. + \left( \frac{2\theta\bar{\lambda}_{\max}(P_0)^2}{\lambda_{\max}(Q_0)} - \frac{\mu}{2}\mu_d \right) \sup_{0 \leq \zeta \leq t} d(\zeta)^2 \right] \psi(t). \end{aligned} \quad (98)$$

Choosing positive constants  $\mu_W, \mu_d, \theta$  in ETM such that they satisfy

$$\mu_W \geq \frac{2r_1\lambda_W}{\mu} \quad (99)$$

$$\mu_d \geq \frac{2r_1\lambda_d}{\mu} \quad (100)$$

$$\theta \leq \min \left\{ \frac{\mu\mu_W}{3\lambda_{\max}(Q_0)}, \frac{\mu_d\mu\lambda_{\max}(Q_0)}{4\bar{\lambda}_{\max}(P_0)^2} \right\} \quad (101)$$

we get

$$\begin{aligned} \dot{\psi}(t) &\leq \frac{\frac{1}{r_1}d(t)^2 - \frac{\mu}{2}\eta m(t)}{\theta\hat{W}^T(t)P_0\hat{W}(t) - \frac{\mu}{2}m(t)} \\ &\quad + \frac{-\frac{\mu}{2}\eta m(t)}{\theta\hat{W}^T(t)P_0\hat{W}(t) - \frac{\mu}{2}m(t)}\psi(t). \end{aligned} \quad (102)$$

Applying the following inequalities:

$$\begin{aligned} \frac{-\frac{\mu}{2}\eta m(t)}{\theta\hat{W}^T(t)P_0\hat{W}(t) - \frac{\mu}{2}m(t)} &\leq \frac{-\frac{\mu}{2}\eta m(t)}{-\frac{\mu}{2}m(t)} = \eta \\ \frac{d(t)^2}{\theta\hat{W}^T(t)P_0\hat{W}(t) - \frac{\mu}{2}m(t)} &= \frac{d(t)^2 + \frac{\mu}{2}m(t) - \frac{\mu}{2}m(t)}{\theta\hat{W}^T(t)P_0\hat{W}(t) - \frac{\mu}{2}m(t)} \\ &\leq \psi(t) + 1 \end{aligned}$$

which hold because of  $m(t) < 0$ , then the inequality (102) becomes

$$\dot{\psi}(t) \leq \frac{1}{r_1} + \eta + \left( \frac{1}{r_1} + \eta \right) \psi(t). \quad (103)$$

It follows that the time needed by  $\psi(t)$  to go from 0 to 1 is at least:

$$\tau = \int_0^1 \frac{1}{\left( \frac{1}{r_1} + \eta \right) \bar{s} + \frac{1}{r_1} + \eta} d\bar{s} > 0 \quad (104)$$

which is independent of initial conditions, where  $\eta$  is a free design parameter appearing in (86) and the condition on the positive constant  $r_1$  from Young's inequality will be determined later.  $\blacksquare$

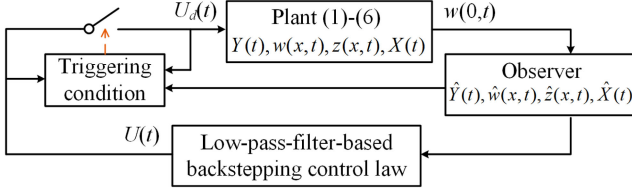


Fig. 2. Event-based output-feedback closed-loop system.

## VI. STABILITY ANALYSIS OF THE EVENT-BASED CLOSED-LOOP SYSTEM

The event-based output-feedback closed-loop system is built as Fig. 2, where a low-pass-filter-based backstepping control law  $U(t)$  in (71), using the states from the observer, is updated at time instants  $t_k$  determined by ETM (85), (86) realized based on the observer, to regulate the PDE plant (1)–(6).

*Lemma 4:* With arbitrary initial data  $(\hat{Y}(0), \hat{z}(x, 0), \hat{w}(x, 0), \hat{X}(0)) \in \chi$ , in the event-based state-feedback loop, the exponential convergence is achieved in the sense that there exist positive constants  $\Upsilon_f, \lambda_f$  such that

$$\hat{\Xi}(t) \leq \Upsilon_f \hat{\Xi}(0) e^{-\lambda_f t} \quad (105)$$

where

$$\begin{aligned} \hat{\Xi}(t) = & \left| \hat{X}(t) \right|^2 + \left| \hat{Y}(t) \right|^2 + \|\hat{z}(\cdot, t)\|^2 + \|\hat{w}(\cdot, t)\|^2 \\ & + |m(t)| + \bar{U}(t)^2. \end{aligned} \quad (106)$$

*Proof:* The state of the low-pass filter is  $\bar{U}(t)$  in (66). According to (63), we have  $\bar{U}(s) = -F(s)C_0\hat{W}(s)$  where  $F(s)$  (67) is a stable, proper transfer function guaranteeing the BIBO property with the estimate as

$$\bar{U}(t)^2 \leq \lambda_{lp}|C_0|^2 \sup_{0 \leq \zeta \leq t} \left| \hat{W}(\zeta) \right|^2 \quad (107)$$

where the positive constant  $\lambda_{lp}$  is associated with the  $L_1$  norm of the impulse response of  $F(s)$ .

Let us consider the Lyapunov function

$$\begin{aligned} V(t) = & r_w \hat{X}(t)^T P \hat{X}(t) + \hat{W}(t)^T P_0 \hat{W}(t) \\ & + \frac{1}{2} r_a \int_0^1 e^{\delta_1 x} \beta(x, t)^2 dx \\ & + \frac{1}{2} r_b \int_0^1 e^{-\delta_2 x} \alpha(x, t)^2 dx - m(t) \end{aligned} \quad (108)$$

where a positive definite matrix  $P = P^T$  is the solution to the Lyapunov equation

$$\hat{A}^T P + P \hat{A} = -Q \quad (109)$$

for some  $Q = Q^T > 0$ . The positive constants  $r_a, r_b, \delta_1, \delta_2, r_w$  are to be determined later. The Lyapunov function (108) is positive definite because of  $m(t) < 0$ .

Defining

$$\begin{aligned} \Omega_0(t) = & \|\alpha(\cdot, t)\|^2 + \|\beta(\cdot, t)\|^2 + \left| \hat{X}(t) \right|^2 \\ & + \left| \hat{W}(t) \right|^2 + |m(t)|. \end{aligned} \quad (110)$$

Recalling (108), (110), the following inequality holds:

$$\mu_1 \Omega_0(t) \leq V(t) \leq \mu_2 \Omega_0(t) \quad (111)$$

for positive constants

$$\mu_1 = \min \left\{ r_w \lambda_{\min}(P), \lambda_{\min}(P_0), \frac{1}{2} r_a, \frac{1}{2} r_b e^{-\delta_2}, 1 \right\} \quad (112)$$

$$\mu_2 = \max \left\{ r_w \lambda_{\max}(P), \lambda_{\max}(P_0), \frac{1}{2} r_a e^{\delta_1}, \frac{1}{2} r_b, 1 \right\}. \quad (113)$$

Taking the derivative of (108) along (79)–(84), recalling (86), one obtain

$$\begin{aligned} \dot{V}(t) = & -r_w \hat{X}(t)^T Q \hat{X}(t) + 2r_w \hat{X}^T P B \alpha(1, t) \\ & - \hat{W}(t)^T Q_0 \hat{W}(t) + 2\hat{W}^T P_0 \mathcal{D}(d(t)) \\ & + \frac{1}{2} q_2 r_a e^{\delta_1} \beta(1, t)^2 - \frac{1}{2} q_2 r_a \beta(0, t)^2 \\ & - \frac{1}{2} \delta_1 q_2 r_a \int_0^1 e^{\delta_1 x} \beta(x, t)^2 dx \\ & - \frac{1}{2} q_1 r_b e^{-\delta_2} \alpha(1, t)^2 + \frac{1}{2} q_1 r_b \left| C_0 \hat{W}(t) \right|^2 \\ & - \frac{1}{2} \delta_2 q_1 r_b \int_0^1 e^{-\delta_2 x} \alpha(x, t)^2 dx \\ & - r_a c_2 \int_0^1 e^{\delta_1 x} \beta(x, t)^2 dx - r_b c_1 \int_0^1 e^{-\delta_2 x} \alpha(x, t)^2 dx \\ & + \eta m(t) + \mu_W \sup_{0 \leq \zeta \leq t} \left| \hat{W}(\zeta) \right|^2 + \mu_d \sup_{0 \leq \zeta \leq t} d(\zeta)^2. \end{aligned} \quad (114)$$

Applying Young's inequality recalling (78), we obtain

$$\begin{aligned} \dot{V}(t) \leq & -\frac{r_w}{2} \lambda_{\min}(Q) \left| \hat{X}(t) \right|^2 \\ & - \left( \frac{1}{2} \lambda_{\min}(Q_0) - \frac{1}{2} q_1 r_b |C_0|^2 \right) \left| \hat{W}(t) \right|^2 \\ & - \left( \frac{1}{2} q_1 r_b e^{-\delta_2} - \frac{2r_w |PB|^2}{\lambda_{\min}(Q)} - \frac{1}{2} q_2 r_a e^{\delta_1} q^2 \right) \alpha(1, t)^2 \\ & - \frac{1}{2} q_2 r_a \beta(0, t)^2 + \frac{2\bar{d} \lambda_{\max}(P_0)^2}{\lambda_{\min}(Q_0)} \sup_{0 \leq \zeta \leq t} d(\zeta)^2 \\ & - \left( \frac{1}{2} \delta_1 q_2 r_a - r_a |c_2| \right) \int_0^1 e^{\delta_1 x} \beta(x, t)^2 dx \\ & - \left( \frac{1}{2} \delta_2 q_1 r_b - r_b |c_1| \right) \int_0^1 e^{-\delta_2 x} \alpha(x, t)^2 dx \\ & - \eta |m(t)| + \mu_W \sup_{0 \leq \zeta \leq t} \left| \hat{W}(\zeta) \right|^2 + \mu_d \sup_{0 \leq \zeta \leq t} d(\zeta)^2. \end{aligned}$$

Choosing  $\delta_1, \delta_2, r_a, r_b, r_w$  as

$$\delta_1 > \frac{2|c_2|}{q_2} \quad (115)$$

$$\delta_2 > \frac{2|c_1|}{q_1} \quad (116)$$

$$r_b < \frac{\lambda_{\min}(Q_0)}{q_1 |C_0|^2} \quad (117)$$

$$r_w < \frac{q_1 r_b e^{-\delta_2} \lambda_{\min}(Q)}{8|PB|^2} \quad (118)$$

$$r_a < \frac{q_1 r_b}{2q_2 q^2} e^{-(\delta_2 + \delta_1)} \quad (119)$$

we, thus, arrive at

$$\begin{aligned} \dot{V}(t) \leq & -\sigma_a V(t) + \mu_W \sup_{0 \leq \zeta \leq t} |\hat{W}(\zeta)|^2 \\ & + \left( \mu_d + \frac{2\bar{\lambda}_{\max}(P_0)^2}{\lambda_{\min}(Q_0)} \right) \sup_{0 \leq \zeta \leq t} d(\zeta)^2 \end{aligned} \quad (120)$$

where

$$\begin{aligned} \sigma_a = \frac{1}{\mu_2} \min \left\{ \frac{r_w}{2} \lambda_{\min}(Q), \frac{1}{2} \lambda_{\min}(Q_0) - \frac{1}{2} q_1 r_b |C_0|^2, \right. \\ \left. \frac{1}{2} \delta_1 q_2 r_a - r_a |c_2|, \left( \frac{1}{2} \delta_2 q_1 r_b - r_b |c_1| \right) e^{-\delta_2}, \eta \right\} > 0. \end{aligned} \quad (121)$$

Multiplying both sides of (120) by  $e^{\sigma_a t}$ , we have

$$\begin{aligned} & e^{\sigma_a t} \dot{V}(t) + e^{\sigma_a t} \sigma_a V(t) \\ \leq & e^{\sigma_a t} \mu_W \sup_{0 \leq \zeta \leq t} |\hat{W}(\zeta)|^2 \\ & + e^{\sigma_a t} \left( \mu_d + \frac{2\bar{\lambda}_{\max}(P_0)^2}{\lambda_{\min}(Q_0)} \right) \sup_{0 \leq \zeta \leq t} d(\zeta)^2. \end{aligned} \quad (122)$$

The left-hand side of (122) is  $\frac{d(e^{\sigma_a t} V(t))}{dt}$ . Integration of (122) from 0 to  $t$  yields

$$\begin{aligned} V(t) \leq & V(0) e^{-\sigma_a t} + \frac{1}{\sigma_a} (1 - e^{-\sigma_a t}) \left[ \mu_W \sup_{0 \leq \zeta \leq t} |\hat{W}(\zeta)|^2 \right. \\ & \left. + \left( \mu_d + \frac{2\bar{\lambda}_{\max}(P_0)^2}{\lambda_{\min}(Q_0)} \right) \sup_{0 \leq \zeta \leq t} d(\zeta)^2 \right] \\ \leq & V(0) e^{-\sigma_a t} + \frac{1}{\sigma_a} \left[ \mu_W \sup_{0 \leq \zeta \leq t} |\hat{W}(\zeta)|^2 \right. \\ & \left. + \left( \mu_d + \frac{2\bar{\lambda}_{\max}(P_0)^2}{\lambda_{\min}(Q_0)} \right) \sup_{0 \leq \zeta \leq t} d(\zeta)^2 \right]. \end{aligned} \quad (123)$$

The triggering condition (85) guarantees

$$\sup_{0 \leq \zeta \leq t} d(\zeta)^2 \leq \theta \lambda_{\max}(P_0) \sup_{0 \leq \zeta \leq t} |\hat{W}(\zeta)|^2 + \mu \sup_{0 \leq \zeta \leq t} |m(\zeta)|. \quad (124)$$

Inserting (124) into (123), and then recalling (110), (111), yields

$$\begin{aligned} V(t) \leq & V(0) e^{-\sigma_a t} + \frac{1}{\sigma_a} \left[ \mu_W \sup_{0 \leq \zeta \leq t} |\hat{W}(\zeta)|^2 \right. \\ & \left. + \left( \mu_d + \frac{2\bar{\lambda}_{\max}(P_0)^2}{\lambda_{\min}(Q_0)} \right) \right. \\ & \left. \times \sup_{0 \leq \zeta \leq t} \left( \theta \lambda_{\max}(P_0) |\hat{W}(\zeta)|^2 + \mu |m(\zeta)| \right) \right] \\ \leq & V(0) e^{-\sigma_a t} \\ & + \frac{1}{\sigma_a} \left[ \mu_W + \left( \mu_d + \frac{2\bar{\lambda}_{\max}(P_0)^2}{\lambda_{\min}(Q_0)} \right) \theta \lambda_{\max}(P_0) \right] \end{aligned}$$

$$\begin{aligned} & \times \sup_{0 \leq \zeta \leq t} |\hat{W}(\zeta)|^2 \\ & + \frac{1}{\sigma_a} \left( \mu_d + \frac{2\bar{\lambda}_{\max}(P_0)^2}{\lambda_{\min}(Q_0)} \right) \mu \sup_{0 \leq \zeta \leq t} |m(\zeta)| \\ \leq & V(0) e^{-\sigma_a t} \\ & + \max \left\{ \frac{1}{\sigma_a} \left[ \mu_W \right. \right. \\ & \left. \left. + \left( \mu_d + \frac{2\bar{\lambda}_{\max}(P_0)^2}{\lambda_{\min}(Q_0)} \right) \theta \lambda_{\max}(P_0) \right], \right. \\ & \left. \frac{1}{\sigma_a} \left( \mu_d + \frac{2\bar{\lambda}_{\max}(P_0)^2}{\lambda_{\min}(Q_0)} \right) \mu \right\} \sup_{0 \leq \zeta \leq t} \Omega_0(\zeta) \\ \leq & V(0) e^{-\sigma_a t} + \bar{\Phi} \sup_{0 \leq \zeta \leq t} V(\zeta) \end{aligned} \quad (125)$$

where

$$\begin{aligned} \bar{\Phi} = & \frac{1}{\mu_1} \max \left\{ \frac{1}{\sigma_a} \mu_W + \frac{1}{\sigma_a} \left( \mu_d + \frac{2\bar{\lambda}_{\max}(P_0)^2}{\lambda_{\min}(Q_0)} \right) \theta \lambda_{\max}(P_0), \right. \\ & \left. \frac{\mu_d \mu}{\sigma_a} + \frac{2\mu \bar{\lambda}_{\max}(P_0)^2}{\sigma_a \lambda_{\min}(Q_0)} \right\}. \end{aligned} \quad (126)$$

In order to ensure that

$$\bar{\Phi} < 1 \quad (127)$$

with combining the conditions (99)–(101) used in avoiding the Zeno phenomenon, the design parameters  $\mu, \mu_d, \mu_W, \theta$  are chosen according to the following guidelines.

1) Choose  $\mu$  as

$$\mu < \frac{\mu_1 \sigma_a \lambda_{\min}(Q_0)}{4\bar{\lambda}_{\max}(P_0)^2} \quad (128)$$

to ensure that  $\frac{2\mu \bar{\lambda}_{\max}(P_0)^2}{\sigma_a \lambda_{\min}(Q_0)} < \frac{\mu_1}{2}$  in (126). Before showing the guidelines for the other design parameters, we define the analysis parameter  $r_1$ , which is from Young's inequality applied in (97), as

$$r_1 < \min \left\{ \frac{\mu_1 \sigma_a}{4\lambda_d}, \frac{\mu \mu_1 \sigma_a}{4\lambda_W} \right\}. \quad (129)$$

The choice of  $r_1$  comes from the need to guarantee that both (127) and (99), (100) hold, which will be seen clearly later.

2) Choose  $\mu_d$  to satisfy

$$\frac{2r_1 \lambda_d}{\mu} \leq \mu_d < \frac{\mu_1 \sigma_a}{2\mu} \quad (130)$$

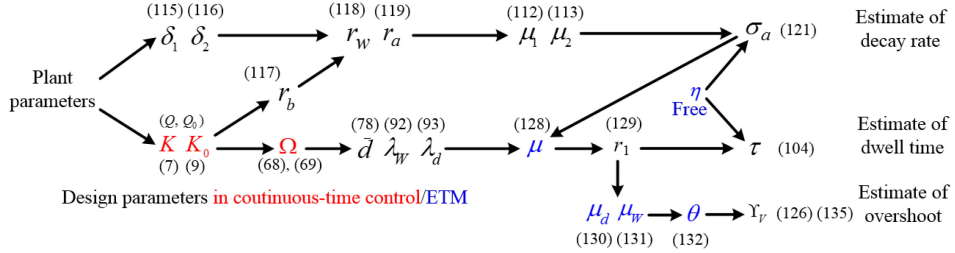
in order to ensure that  $\frac{\mu_d \mu}{\sigma_a} < \frac{\mu_1}{2}$  in (126) (with the right inequality of (130)). Recalling (128), the final term in (126) is less than  $\mu_1$ . The condition (100) is incorporated as the left inequality of (130).

3) Choose  $\mu_W$  to satisfy

$$\frac{2r_1 \lambda_W}{\mu} \leq \mu_W < \frac{\mu_1 \sigma_a}{2} \quad (131)$$

in order to ensure that  $\frac{1}{\sigma_a} \mu_W < \frac{\mu_1}{2}$  in (126) (with the right inequality of (131)), where the condition (99) is incorporated as the left inequality of (131).

The parameter  $r_1$  (129) is chosen to ensure that the far left terms of (130), (131) are less than the far right ones, where the far right terms are from ensuring (127) and the far left terms are from the conditions (99), (100) on avoiding the Zeno phenomenon.



3) Rewriting the observer states in the output-feedback control input as a sum of the plant states and the observer errors according to (18), inserting the result into the plant (1)–(6), through the same steps as in the above state-feedback control designs, it follows that the closed-loop dynamics are a cascade of the observer error dynamics feeding into the target system dynamics in the form of (79)–(84) (the state-feedback loop). Because the stability of the observer error dynamics (which depends on the choices of  $L, L_0$ ) and the stability of the state-feedback loop dynamics (which depends on the choices of  $K, K_0$ ) are independent, the separation principle holds. Equation (140) is, thus, obtained recalling Lemma 1 and Lemma 4, where the overshoot  $\Upsilon_a$  is associated with  $\Upsilon_e, \Upsilon_f$  and the decay rate  $\sigma_a$  is associated with  $\lambda_e, \lambda_f$ .

4) Recalling (71) and the stability result proved in property 3), we have the continuous-in-time control input  $U(t)$  is convergent to zero. According to the definition (72), property 4) is obtained. ■

## VII. APPLICATION IN MINING CABLE ELEVATOR

In this section, the proposed event-triggered backstepping boundary control design is applied to axial vibration control of a mining cable elevator that is 2000 m deep, and whose dynamics include the hydraulic actuator, mining cable, and cage.

### A. Model

The vibration model of the mining cable elevator is described by a wave PDE [44], [46] sandwiched by two ODEs

$$M_h \ddot{b}_0(t) = -c_h \dot{b}_0(t) + \frac{\pi R_d^2}{4} E u_x(0, t) + U_d(t) \quad (142)$$

$$u(0, t) = b_0(t) \quad (143)$$

$$\rho u_{tt}(x, t) = \frac{\pi R_d^2}{4} E u_{xx}(x, t) - d_c u_t(x, t), \quad x \in [0, \bar{L}] \quad (144)$$

$$u(\bar{L}, t) = b_L(t) \quad (145)$$

$$M_c \ddot{b}_L(t) = -c_L \dot{b}_L(t) + \frac{\pi R_d^2}{4} E u_x(\bar{L}, t) \quad (146)$$

where  $U_d(t)$  is the event-triggered backstepping control input of the electronically controlled valves, which regulates the hydraulic actuator to suppress vibrations of the mining cable elevator according to Fig. 2. The PDE state  $u(x, t)$  denotes distributed axial vibration dynamics along the cable. The ODE state  $b_0(t)$  represents the displacement of the hydraulic actuator and  $b_L(t)$  is the vibration displacement of the cage. The physical parameters in (142)–(146) of the mining cable elevator are shown in Table I. We apply the Riemann transformations

$$z(x, t) = u_t(x, t) - \sqrt{\frac{E\pi}{\rho}} \frac{R_d}{2} u_x(x, t) \quad (147)$$

$$w(x, t) = u_t(x, t) + \sqrt{\frac{E\pi}{\rho}} \frac{R_d}{2} u_x(x, t) \quad (148)$$

TABLE I  
PHYSICAL PARAMETERS OF THE MINING CABLE ELEVATOR

Parameters (units)	values
Depth $\bar{L}$ (m)	2000
Cable diameter $R_d$ (m)	0.2
Cable effective Young Modulus $E$ (N/m <sup>2</sup> )	$1.02 \times 10^9$
Cable linear density $\rho$ (kg/m)	8.1
Mass of hydraulic actuator $M_h$ (kg)	300
Mass of cage $M_c$ (kg)	15000
Damping coefficient of hydraulic actuator $c_h$	0.4
Damping coefficient of cage $c_L$	0.4
Cable material damping coefficient $d_c$	0.5
Gravitational acceleration $g$ (m/s <sup>2</sup> )	9.8

and define the new variables  $Y(t) = \dot{b}_0(t), X(t) = \dot{b}_L(t)$ , which allows us to rewrite (142)–(146) as (1)–(6), with

$$q_1 = q_2 = \sqrt{\frac{E\pi}{\rho}} \frac{R_d}{2}, \quad c_1 = c_2 = \frac{-d_c}{2\rho} \quad (149)$$

$$q = p = -1, \quad C_0 = C_1 = 2 \quad (150)$$

$$A_0 = \frac{-c_h}{M_h} - \frac{R_d \sqrt{E\pi\rho}}{2M_h}, \quad E_0 = \frac{R_d \sqrt{E\pi\rho}}{2M_h}, \quad B_0 = \frac{1}{M_h} \quad (151)$$

$$A = \frac{-c_L}{M_c} + \frac{R_d \sqrt{E\pi\rho}}{2M_c}, \quad B = -\frac{R_d \sqrt{E\pi\rho}}{2M_c}. \quad (152)$$

Assumptions 1–3 are satisfied with (149)–(152). Initial conditions of  $z(x, t)$  and  $w(x, t)$  are defined as  $z(x, 0) = 0.01 \sin(2\pi(\bar{L} - x)/\bar{L} + \pi/6)$ ,  $w(x, 0) = 0.01 \sin(3\pi(\bar{L} - x)/\bar{L})$  and  $X(0) = \frac{1}{2}(w(\bar{L}, 0) - qz(\bar{L}, 0))$ ,  $Y(0) = \frac{1}{2}(z(0, 0) - pw(0, 0))$ , according to (5). The observer initial conditions are defined as  $\hat{z}(x, 0) = z(x, 0) + 0.2$ ,  $\hat{w}(x, 0) = w(x, 0) + 0.2$  where 0.2 is an initial observe error,  $\hat{X}(0) = \frac{1}{2}(\hat{w}(\bar{L}, 0) - q\hat{z}(\bar{L}, 0))$ ,  $\hat{Y}(0) = \frac{1}{2}(\hat{z}(0, 0) - p\hat{w}(0, 0))$ , according to (16). We pick the initial value of  $m(t)$  as  $m(0) = -0.001$ . The simulation is conducted based on the finite difference method with the time step of 0.0015 s and the space step of 0.5 m.

### B. Determination of Design Parameters

The free design parameter  $\eta$  in (86) is selected as  $\eta = 0.11$ . The parameters affecting the decay rate of the states in the closed-loop system are determined as follows. According to  $A_0, A, B_0, B, C_0, C$  in (150)–(152) and the parameter values in Table I, recalling (7)–(10), the control gains and observer gains are chosen as  $K_0 = 1$ ,  $K = 1.5$  and  $L_0 = 1$ ,  $L = 2$ , respectively, yielding  $\hat{A}_0 = -106.7$ ,  $\hat{A} = -1.067$ ,  $\bar{A} = -2.9$ ,  $\bar{A}_0 = -55.4$ . Defining  $P = P_0 = \frac{1}{2}$ , we then have  $\lambda_{\min}(Q_0) = 106.7$ ,  $\lambda_{\min}(Q) = 1.067$  via (88), (109). Considering (68), (69), and  $C_0(I_s - \hat{A}_0)^{-1}B_0 = \frac{2}{300(s+106.7)}$  in  $F(s)$  in (67), the low-pass filter is chosen as the first-order type  $\Omega(s) = \frac{1}{1+0.0011s}$ , which can be implemented with an RC circuit. Next, choosing  $\delta_1 = 0.5$ ,  $\delta_2 = 0.5$  according to (115) and (116), and then determining  $r_b = 0.013$ ,  $r_w = 7.3$ ,  $r_a = 0.0023$  from (117)–(119), leads to  $\mu_2 = 3.65$ ,  $\mu_1 = 0.0011$  according to the formulate (112), (113). Therefore, the estimate of the decay rate  $\sigma_a$  obtained from (121) is 0.108.

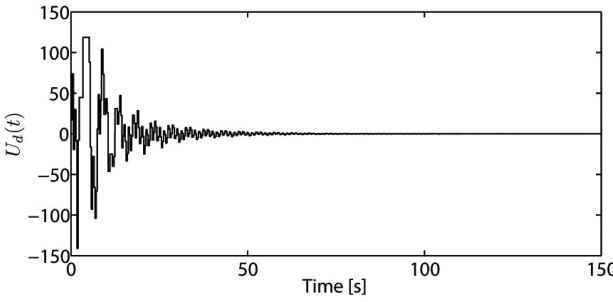


Fig. 4. Output-feedback event-based control input  $U_d(t)$ .

The parameters of ETM are determined as follows. According to the transfer functions (77), (92), (93), the plant parameters, and the choices of  $K_0$ ,  $K$ , a group of conservative estimates of  $\bar{d}$ ,  $\lambda_W$ ,  $\lambda_d$  is  $\bar{d} = 5$ ,  $\lambda_W = 250$ ,  $\lambda_d = 600$ . Recalling (128), (129),  $\mu$  is defined as  $\mu = 0.0024$  and  $r_1$  as  $r_1 = 0.22 \times 10^{-9}$ . Then,  $\mu_W$ ,  $\mu_d$  are determined by (130) and (131) as  $\mu_d = 0.01$ ,  $\mu_W = 0.5 \times 10^{-4}$ . Finally, pick  $\theta = 0.36 \times 10^{-9}$  via (132). Recalling (104) for the highly conservative minimal dwell-time estimate  $\tau$ , we get  $\tau = 0.15 \times 10^{-9}$  s. Substituting the above-mentioned parameters into (126), we arrive at  $\bar{\Phi} = 0.6754$ .

The approximate solutions of the kernels  $M(x, y)$ ,  $N(x, y)$ ,  $\gamma(x)$ ,  $H(x, y)$ ,  $J(x, y)$ ,  $\lambda(x)$  are obtained from the conditions (B.1)–(B.12), which are two groups of coupled linear hyperbolic PDE-ODE systems on the domain  $\{(x, y) | 0 \leq x \leq y \leq \bar{L}\}$ . The finite difference method is employed, with a step length of 0.5 m for  $y$  running from  $x$  to  $\bar{L}$ . The approximate solutions of  $\bar{K}_1(x)$ ,  $\bar{K}_2(x)$ ,  $\bar{K}_3$ ,  $\bar{K}_4(x)$ ,  $\bar{K}_5(x)$ ,  $\bar{K}_6$  are obtained from conditions (C.1)–(C.6) by the finite difference method w.r.t.  $x \in [0, \bar{L}]$ . Based on the abovementioned approximate solutions,  $N_1$ ,  $N_2$ ,  $M_\alpha(x)$ ,  $M_\beta(x)$ ,  $M_X$  are obtained using (D.1)–(D.5).

### C. Closed-Loop Responses

Fig. 4 shows the event-triggered control input, where the minimal dwell-time is 0.297 s, which is much larger than the conservative estimate  $\tau = 0.15 \times 10^{-9}$  of the minimal dwell-time. If the design parameter  $\eta$  is picked as a smaller one 0.106 (other design parameters are not changed), compared with the first value  $\eta = 0.11$  defined in the last section, the number of update times of the control input decreases from 373 to 361, i.e., the actuation frequency is further reduced. However, the control performance is slightly degraded because  $\eta$  also affects the convergence rate of the closed-loop system. The result of  $\theta \hat{W}^T(t) P_0 \hat{W}(t) - \mu m(t) - d(t)^2$  is shown in Fig. 5, from which we can see that  $d(t)^2 \leq \theta \hat{W}^T(t) P_0 \hat{W}(t) - \mu m(t)$  is guaranteed all the time. The time evolution of the internal dynamic variable  $m(t)$  is given in Fig. 6, which shows  $m(t) < 0$ . Fig. 7 shows the convergence of the ODE states  $X(t)$ ,  $Y(t)$ , i.e., the suppression of the axial vibration velocity of the cage and the regulation of the moving velocity of the hydraulic rod in the hydraulic cylinder at the head sheaves. Integrations of  $X(t)$ ,  $Y(t)$ , i.e., the axial vibration displacement of the cage and the movement of the hydraulic rod in the hydraulic cylinder, are shown in Fig. 8 under the initial elastic displacement of 0.005 m at the

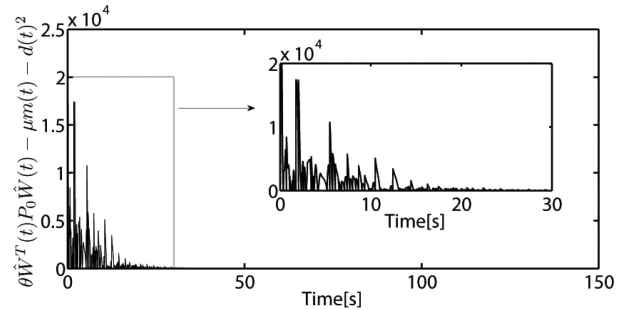


Fig. 5. Result of  $\theta \hat{W}^T(t) P_0 \hat{W}(t) - \mu m(t) - d(t)^2$ .

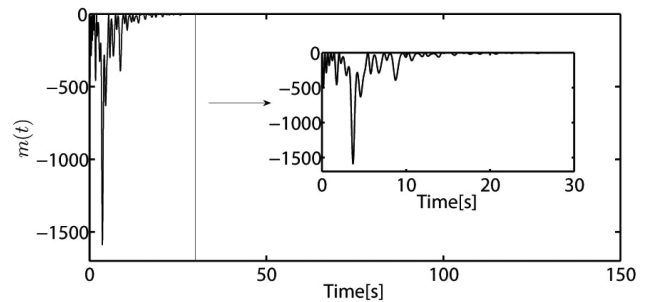


Fig. 6. Internal dynamic variable  $m(t)$ .

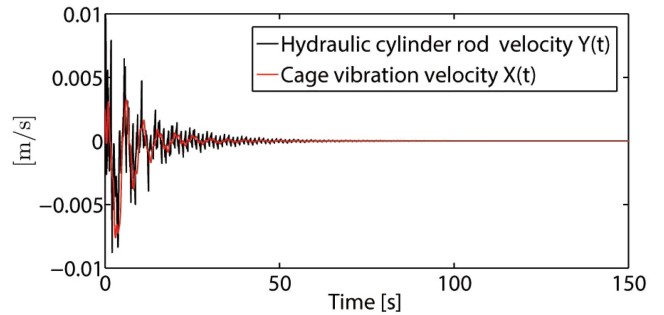


Fig. 7. Axial vibration velocity of the cage  $X(t)$  and moving velocity of the hydraulic rod in the hydraulic cylinder  $Y(t)$ .

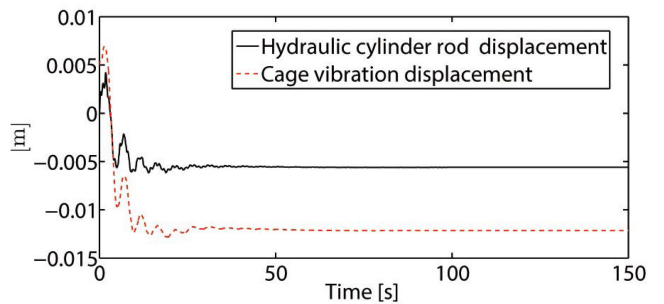


Fig. 8. Axial vibration displacement of the cage (initial elastic displacement 0.005 m) and movement of the hydraulic rod in the hydraulic cylinder (initial position 0.001 m).

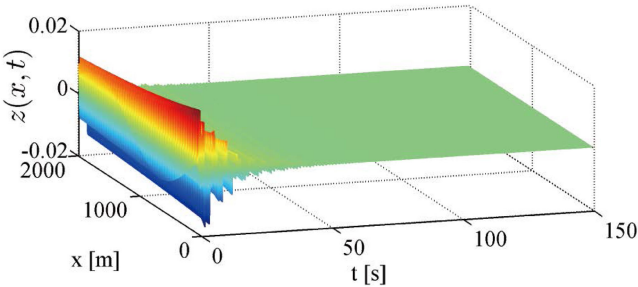


Fig. 9. Response of  $z(x, t)$ .

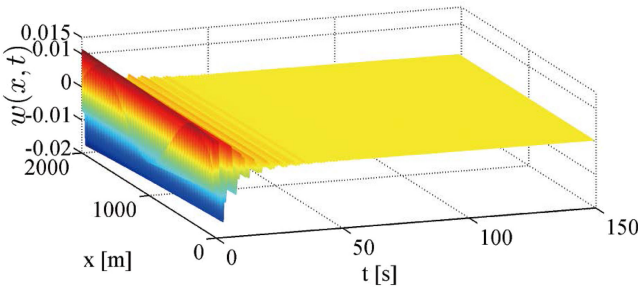


Fig. 10. Response of  $w(x, t)$ .

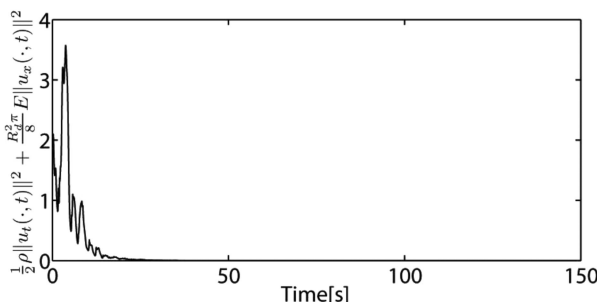


Fig. 11. Axial vibration energy  $V_E$  of the cable.

cable-cage connection point, and the initial position 0.001 m of the hydraulic rod. Figs. 9 and 10 show the convergence of the PDE states  $z(x, t), w(x, t)$ . The axial vibration energy of the cable,  $V_E = \frac{1}{2}\rho\|u(\cdot, t)\|^2 + \frac{R_d^2\pi E}{8}\|u_x(\cdot, t)\|^2$  is converted into  $V_E = \frac{ER_d^2}{8\pi E\pi\rho R_d^2}\|z(\cdot, t) - w(\cdot, t)\|^2 + \frac{\rho}{8}\|z(\cdot, t) + w(\cdot, t)\|^2$  using (147) and (148). It is observed from Fig. 11 that the axial vibration energy of the cable is reduced with the help of the proposed event-based vibration control system.

## VIII. CONCLUSION

In this article, an event-triggered output-feedback backstepping boundary controller for an ODE- $2 \times 2$  hyperbolic PDE-ODE system is proposed. An observer design using only one measurement at the PDE actuated boundary and a two-step control design, including the design of a low-pass-filter-based backstepping continuous-in-time boundary control law, and the subsequent design of an ETM, which determines triggering times of updating the obtained continuous-in-time control law,

are proposed. The existence of a minimal dwell-time between two triggering times and the achievement of exponential convergence in the event-based output-feedback closed-loop system are proved. The proposed event-based controller is applied into axial vibration control of a mining cable elevator consisting of the hydraulic-driven head sheaves, mining cable, and cage in the simulation, where the results show the controller effectively suppresses the axial vibration energy and the actual minimal dwell-time between two triggering times is much larger than the conservative estimate one. In future work, an event-based observer and a time-varying PDE domain according to the time-varying length of cable in the ascending/descending process will be considered in the control design.

## APPENDIX

A. The functions  $\bar{\phi}, \bar{\phi}_1, \bar{\psi}, \bar{\psi}_1$  on  $\{(x, y) | 0 \leq y \leq x \leq 1\}$  and  $\bar{\gamma}, \bar{\varphi}$  on  $\{0 \leq x \leq 1\}$ , in (19), (20), satisfy

$$-q_1\bar{\phi}_x(x, y) - q_1\bar{\phi}_y(x, y) - c_1\bar{\psi}(x, y) = 0 \quad (\text{A.1})$$

$$q_2\bar{\psi}_x(x, y) - q_1\bar{\psi}_y(x, y) \quad (\text{A.2})$$

$$-(c_2 - c_1)\bar{\psi}(x, y) - c_2\bar{\phi}(x, y) = 0 \quad (\text{A.3})$$

$$\bar{\phi}(1, y) = \frac{1}{q}CK_1(y) + \frac{1}{q}\bar{\psi}(1, y) \quad (\text{A.4})$$

$$\bar{\psi}(x, x) = -\frac{c_2}{q_1 + q_2} \quad (\text{A.5})$$

$$q_2\bar{\phi}_{1y}(x, y) - q_1\bar{\phi}_{1x}(x, y) \quad (\text{A.6})$$

$$+ (c_2 - c_1)\bar{\phi}_1(x, y) - c_1\bar{\psi}_1(x, y) = 0 \quad (\text{A.7})$$

$$q_2\bar{\psi}_{1y}(x, y) + q_2\bar{\psi}_{1x}(x, y) - c_2\bar{\phi}_1(x, y) = 0 \quad (\text{A.8})$$

$$\bar{\psi}_1(1, y) = q\bar{\phi}_1(1, y) - CK_2(y) \quad (\text{A.9})$$

$$\bar{\phi}_1(x, x) = \frac{c_1}{q_1 + q_2} \quad (\text{A.10})$$

$$-q_2\bar{\varphi}'(x) + \bar{\varphi}(x)\bar{A}_0 + c_2\bar{\gamma}(x) + c_2\bar{\varphi}(x) = 0 \quad (\text{A.11})$$

$$q_1\bar{\gamma}'(x) + \bar{\gamma}(x)\bar{A}_0 + c_1\bar{\gamma}(x) + c_1\bar{\varphi}(x) = 0 \quad (\text{A.12})$$

and  $K_1(y), K_2(y)$  are the solutions of the following ODEs:

$$-q_1K_1'(y) + AK_1(y) + c_1K_1(y) - B\bar{\phi}(1, y) = 0 \quad (\text{A.13})$$

$$K_1(1) = \frac{Lq - B}{q_1} \quad (\text{A.14})$$

$$q_2K_2'(y) + AK_2(y) + c_2K_2(y) - B\bar{\phi}_1(1, y) = 0 \quad (\text{A.15})$$

$$K_2(1) = \frac{L}{q_2}. \quad (\text{A.16})$$

Regarding the conditions (A.1)–(A.12), (A.13)–(A.16), sets (A.1)–(A.4), (A.13), (A.14) and (A.5)–(A.8), (A.15), (A.16) are two independent  $2 \times 2$  hyperbolic PDE-ODE systems, whose well-posedness can be obtained following the proof of [43, Lemma 1]. Solving (A.9)–(A.12) is an initial value problem and explicit solutions can be obtained. Therefore, (A.1)–(A.12), (A.13)–(A.16) are well-posed.

B. The conditions of the kernels  $M, N, H, J$  on  $\{(x, y) | 0 \leq x \leq y \leq 1\}$  and  $\gamma, \lambda$  on  $\{0 \leq x \leq 1\}$ , in (31) and (32), are given by

$$q_1 M(x, 1) - q_2 N(x, 1)q - \gamma(x)B = 0 \quad (\text{B.1})$$

$$(q_2 + q_1)N(x, x) - c_1 = 0 \quad (\text{B.2})$$

$$\begin{aligned} c_1 M(x, y) - q_1 N_x(x, y) + q_2 N_y(x, y) \\ + (c_2 - c_1)N(x, y) = 0 \end{aligned} \quad (\text{B.3})$$

$$c_2 N(x, y) - q_1 M_x(x, y) - q_1 M_y(x, y) = 0 \quad (\text{B.4})$$

$$\gamma(1) = -K \quad (\text{B.5})$$

$$-q_1 \gamma'(x) - \gamma(x)A - c_1 \gamma(x) - q_2 N(x, 1)C = 0 \quad (\text{B.6})$$

$$q_1 H(x, 1) - q_2 J(x, 1)q - \lambda(x)B = 0 \quad (\text{B.7})$$

$$-c_2 - (q_1 + q_2)H(x, x) = 0 \quad (\text{B.8})$$

$$c_1 H(x, y) + q_2 J_x(x, y) + q_2 J_y(x, y) = 0 \quad (\text{B.9})$$

$$\begin{aligned} q_2 H_x(x, y) - q_1 H_y(x, y) \\ + c_2 J(x, y) + (c_1 - c_2)H(x, y) = 0 \end{aligned} \quad (\text{B.10})$$

$$q_2 \lambda'(x) - \lambda(x)A - c_2 \lambda(x) - q_2 J(x, 1)C = 0 \quad (\text{B.11})$$

$$q\gamma(1) - \lambda(1) + C = 0. \quad (\text{B.12})$$

C. In (33) and (34),  $\bar{K}_1(x), \bar{K}_2(x), \bar{K}_3, \bar{K}_4(x), \bar{K}_5(x), \bar{K}_6$  are the solutions of the following linear Volterra integral equations of the second kind:

$$\begin{aligned} \bar{K}_1(x) = pH(0, x) - M(0, x) + \int_0^x \bar{K}_1(y)M(y, x)dy \\ + \int_0^x \bar{K}_2(y)H(y, x)dy \end{aligned} \quad (\text{C.1})$$

$$\begin{aligned} \bar{K}_2(x) = -pJ(0, x) + N(0, x) + \int_0^x \bar{K}_1(y)N(y, x)dy \\ + \int_0^x \bar{K}_2(y)J(y, x)dy \end{aligned} \quad (\text{C.2})$$

$$\begin{aligned} \bar{K}_3 = \int_0^1 \bar{K}_2(x)\lambda(x)dx + \int_0^1 \bar{K}_1(x)\gamma(x)dx \\ + p\lambda(0) - \gamma(0) \end{aligned} \quad (\text{C.3})$$

$$\begin{aligned} \bar{K}_4(x) = \int_0^x \bar{K}_4(y)M(y, x)dy + \int_0^x \bar{K}_5(y)H(y, x)dy \\ - E_0 H(0, x) \end{aligned} \quad (\text{C.4})$$

$$\begin{aligned} \bar{K}_5(x) = \int_0^x \bar{K}_4(y)N(y, x)dy + \int_0^x \bar{K}_5(y)J(y, x)dy \\ + E_0 J(0, x) \end{aligned} \quad (\text{C.5})$$

$$\begin{aligned} \bar{K}_6 = \int_0^1 \bar{K}_5(x)\lambda(x)dx + \int_0^1 \bar{K}_4(x)\gamma(x)dx \\ + E_0 \lambda(0). \end{aligned} \quad (\text{C.6})$$

D. Expressions for  $N_1, N_2, M_\alpha, M_\beta, M_X$  are

$$N_1 = C_0^+ \bar{K}_3 B - q_1 C_0^+ \bar{K}_1(1) + q_2 C_0^+ \bar{K}_2(1)q \quad (\text{D.1})$$

$$N_2 = E_0 - q_2 C_0^+ \bar{K}_2(0) + q_1 C_0^+ \bar{K}_1(0)p \quad (\text{D.2})$$

$$M_\alpha(x) = \bar{K}_4(x) + q_1 C_0^+ \bar{K}_1'(x) - (\hat{A}_0 + c_1)C_0^+ \bar{K}_1(x) \quad (\text{D.3})$$

$$M_\beta(x) = \bar{K}_5(x) - q_2 C_0^+ \bar{K}_2'(x) - (\hat{A}_0 + c_2)C_0^+ \bar{K}_2(x) \quad (\text{D.4})$$

$$M_X = C_0^+ \bar{K}_3 \hat{A} + \bar{K}_6 - \hat{A}_0 C_0^+ \bar{K}_3. \quad (\text{D.5})$$

## REFERENCES

- [1] J. Auriol, U. J. F. Aarsnes, P. Martin, and F. Di Meglio, "Delay-robust control design for two heterodirectional linear coupled hyperbolic PDEs," *IEEE Trans. Autom. Control*, vol. 63, no. 10, pp. 3551–3557, Oct. 2018.
- [2] O. M. Aamo, "Disturbance rejection in  $2 \times 2$  linear hyperbolic systems," *IEEE Trans. Autom. Control*, vol. 58, no. 5, pp. 1095–1106, May 2013.
- [3] H. Anfinsen and O. M. Aamo, "Disturbance rejection in general heterodirectional 1-D linear hyperbolic systems using collocated sensing and control," *Automatica*, vol. 76, pp. 230–242, 2017.
- [4] H. Anfinsen and O. M. Aamo, "Adaptive output-feedback stabilization of linear  $2 \times 2$  hyperbolic systems using anti-collocated sensing and control," *Syst. Control Letters*, vol. 104, pp. 86–94, 2017.
- [5] H. Anfinsen and O. M. Aamo, "Adaptive control of linear  $2 \times 2$  hyperbolic systems," *Automatica*, vol. 87, pp. 69–82, 2018.
- [6] H. Anfinsen and O. M. Aamo, "Stabilization of a linear hyperbolic PDE with actuator and sensor dynamics," *Automatica*, vol. 95, pp. 104–111, 2018.
- [7] G. Bastin and J. M. Coron, *Stability and Boundary Stabilization of 1-D Hyperbolic Systems*. Basel, Cambridge, MA, USA: Birkhauser, 2016.
- [8] D. Bou Saba, F. Bribiesca Argomedo, M. Di Loreto, and D. Eberard, "Backstepping stabilization of  $2 \times 2$  linear hyperbolic PDEs coupled with potentially unstable actuator and load dynamics," in *Proc. 56th IEEE Conf. Decis. Control*, 2017, pp. 2498–2503.
- [9] D. Bou Saba, F. Bribiesca-Argomedo, M. D. Loreto, and D. Eberard, "Strictly proper control design for the stabilization of  $2 \times 2$  linear hyperbolic ODE-PDE-ODE systems," in *Proc. 58th IEEE Conf. Decis. Control*, 2019, pp. 4996–5001.
- [10] R. Curtain and K. Morris, "Transfer functions of distributed parameter systems: A tutorial," *Automatica*, vol. 45, no. 5, pp. 1101–1116, 2009.
- [11] J. M. Coron, R. Vazquez, M. Krstic, and G. Bastin, "Local exponential  $H^2$  stabilization of a  $2 \times 2$  quasilinear hyperbolic system using backstepping," *SIAM J. Control Optim.*, vol. 51, no. 3, pp. 2005–2035, 2013.
- [12] M. A. Davo, D. Bresch-Pietri, C. Prieur, and F. Di Meglio, "Stability analysis of a  $2 \times 2$  linear hyperbolic system with a sampled-data controller via backstepping method and looped-functionals," *IEEE Trans. Autom. Control*, vol. 64, no. 4, pp. 1718–1725, Apr. 2019.
- [13] J. Doyle, B. Francis, and A. Tannenbaum, *Feedback Control Theory*, New York, NY, USA: MacMillan, 1992.
- [14] J. Deutscher, "Finite-time output regulation for linear  $2 \times 2$  hyperbolic systems using backstepping," *Automatica*, vol. 75, pp. 54–62, 2017.
- [15] J. Deutscher, "Output regulation for general linear heterodirectional hyperbolic systems with spatially-varying coefficients," *Automatica*, vol. 85, pp. 34–42, 2017.
- [16] J. Deutscher, N. Gehring, and R. Kern, "Output feedback control of general linear heterodirectional hyperbolic ODE-PDE-ODE systems," *Automatica*, vol. 95, pp. 472–480, 2018.
- [17] J. Deutscher, N. Gehring, and R. Kern, "Output feedback control of general linear heterodirectional hyperbolic PDE-ODE systems with spatially-varying coefficients," *Int. J. Control.*, vol. 92, pp. 2274–2290, 2019.
- [18] N. Espitia, A. Girard, N. Marchand, and C. Prieur, "Event-based control of linear hyperbolic systems of conservation laws," *Automatica*, vol. 70, pp. 275–287, 2016.
- [19] N. Espitia, A. Girard, N. Marchand, and C. Prieur, "Event-based stabilization of linear systems of conservation laws using a dynamic triggering condition," in *Proc. 10th IFAC Symp. Nonlinear Control Syst.*, Monterey, CA, USA, 2016, vol. 49, pp. 362–367.
- [20] N. Espitia, A. Girard, N. Marchand, and C. Prieur, "Event-based boundary control of a linear  $2 \times 2$  hyperbolic system via backstepping approach," *IEEE Trans. Autom. Control*, vol. 63, no. 8, pp. 2686–2693, Aug. 2018.

[21] N. Espitia, I. Karafyllis and M. Krstic, "Event-triggered boundary control of constant-parameter reaction-diffusion PDEs: A small-gain approach," 2019, *arXiv:1909.10472*.

[22] N. Espitia, "Observer-based event-triggered boundary control of a linear  $2 \times 2$  hyperbolic systems," *Syst. Control Lett.*, vol. 138, 2020, Art. no. 104668.

[23] E. Fridman and A. Blighovsky, "Robust sampled-data control of a class of semilinear parabolic systems," *Automatica*, vol. 48, no. 5, pp. 826–836, 2012.

[24] A. Girard, "Dynamic triggering mechanisms for event-triggered control," *IEEE Trans. Autom. Control*, vol. 60, no. 7, pp. 1992–1997, Jul. 2015.

[25] W. P. M. H. Heemels, K. H. Johansson, and P. Tabuada, "An introduction to event-triggered and self-triggered control," in *Proc. 51st IEEE Conf. Decis. Control*, Maui, Hawaii, 2012, pp. 3270–3285.

[26] L. Hu, F. Di Meglio, R. Vazquez, and M. Krstic, "Control of homodirectional and general heterodirectional linear coupled hyperbolic PDEs," *IEEE Trans. Autom. Control*, vol. 61, no. 11, pp. 3301–3314, Nov. 2016.

[27] M. Krstic, "Compensation of infinite-dimensional actuator and sensor dynamics: Nonlinear and delay-adaptive systems," *IEEE Control Syst. Mag.*, vol. 30, no. 1, pp. 22–41, Feb. 2010.

[28] M. Krstic, "Lyapunov tools for predictor feedbacks for delay systems: Inverse optimality and robustness to delay mismatch," *Automatica*, vol. 44, no. 11, pp. 2930–2935, 2008.

[29] M. Krstic, *Delay Compensation for Nonlinear, Adaptive, and PDE Systems*, Berlin, Germany: Springer, 2009.

[30] I. Karafyllis and M. Krstic, "Sampled-data boundary feedback control of 1-D parabolic PDEs," *Automatica*, vol. 87, pp. 226–237, 2018.

[31] I. Karafyllis and M. Krstic, "Sampled-data boundary feedback control of 1-D linear transport PDEs with non-local terms," *Syst. Control Lett.*, vol. 107, pp. 68–75, 2017.

[32] W.-J. Liu and M. Krstic, "Backstepping boundary control of burgers' equation with actuator dynamics," *Syst. Control Lett.*, vol. 41, pp. 291–303, 2000.

[33] N. Marchand, S. Durand, and J. F. G. Castellanos, "A general formula for event-based stabilization of nonlinear systems," *IEEE Trans. Autom. Control*, vol. 58, no. 5, pp. 1332–1337, May 2013.

[34] P. J. Moylan, "Stable inversion of linear systems," *IEEE Trans. Autom. Control*, vol. 22, no. 1, pp. 74–78, Feb. 1977.

[35] F. Di Meglio, R. Vazquez, and M. Krstic, "Stabilization of a system of  $n + 1$  coupled first-order hyperbolic linear PDEs with a single boundary input," *IEEE Trans. Autom. Control*, vol. 58, no. 12, pp. 3097–3111, Dec. 2013.

[36] F. Di Meglio, F. Bribiesca, L. Hu, and M. Krstic, "Stabilization of coupled linear heterodirectional hyperbolic PDE-ODE systems," *Automatica*, vol. 87, pp. 281–289, 2018.

[37] F. Di Meglio, P.-O. Lamare, and U. J. F. Aarsnes, "Robust output feedback stabilization of an ODE-PDE-ODE interconnection," *Automatica*, vol. 119, 2020, Art. no. 109059.

[38] C. Prieur, A. Girard, and E. Witran, "Stability of switched linear hyperbolic systems by lyapunov techniques," *IEEE Trans. Autom. Control*, vol. 59, no. 8, pp. 2196–2202, Aug. 2014.

[39] A. Selivanov and E. Fridman, "Distributed event-triggered control of diffusion semilinear PDEs," *Automatica*, vol. 68, pp. 344–351, 2016.

[40] A. Seuret, C. Prieur, and N. Marchand, "Stability of non-linear systems by means of event-triggered sampling algorithms," *IMA J. Math. Control Inf.*, vol. 31, no. 3, pp. 415–433, 2014.

[41] P. Tabuada, "Event-triggered real-time scheduling of stabilizing control tasks," *IEEE Trans. Autom. Control*, vol. 52, no. 9, pp. 1680–1685, Sep. 2007.

[42] R. Vazquez, M. Krstic, and J. M. Coron, "Backstepping boundary stabilization and state estimation of a  $2 \times 2$  linear hyperbolic system," in *Proc. 50th IEEE Conf. Decis. Control and Eur. Control Conf.*, 2011, pp. 4937–4942.

[43] J. Wang, M. Krstic, and Y. Pi, "Control of a  $2 \times 2$  coupled linear hyperbolic system sandwiched between two ODEs," *Int. J. Robust Nonlin.*, vol. 28, pp. 3987–4016, 2018.

[44] J. Wang, S. Koga, Y. Pi, and M. Krstic, "Axial vibration suppression in a PDE model of ascending mining cable elevator," *J. Dyn. Sys., Meas., Control.*, vol. 140, 2018, Art. no. 111003.

[45] J. Wang, S.-X. Tang, Y. Pi, and M. Krstic, "Exponential regulation of the anti-collocatedly disturbed cage in a wave PDE-modeled ascending cable elevator," *Automatica*, vol. 95, pp. 122–136, 2018.

[46] J. Wang, Y. Pi, and M. Krstic, "Balancing and suppression of oscillations of tension and cage in dual-cable mining elevators," *Automatica*, vol. 98, pp. 223–238, 2018.

[47] J. Wang and M. Krstic, "Output-feedback boundary control of a heat PDE sandwiched between two ODEs," *IEEE Trans. Autom. Control*, vol. 64, no. 11, pp. 4653–4660, Nov. 2019.

[48] J. Wang and M. Krstic, "Output-feedback control of an extended class of sandwiched hyperbolic PDE-ODE systems," *IEEE Trans. Autom. Control*, to be published, doi: [10.1109/TAC.2020.3012530](https://doi.org/10.1109/TAC.2020.3012530).

[49] J. Wang and M. Krstic, "Delay-compensated control of sandwiched ODE-PDE-ODE hyperbolic systems for oil drilling and disaster relief," *Automatica*, vol. 120, 2020, Art. no. 109131.

[50] Z. Yao and N. H. El-Farra, "Resource-aware model predictive control of spatially distributed processes using event-triggered communication," in *Proc. 52nd IEEE Conf. Decis. Control*, 2013, pp. 3726–3731.



**Ji Wang** (Member, IEEE) received the Ph.D. degree in mechanical engineering from Chongqing University, Chongqing, China, in 2018.

From 2019, he is a Postdoctoral Scholar-Employee with the Department of Mechanical and Aerospace Engineering, University of California, San Diego, La Jolla, CA, USA. His research interests include modeling and control of distributed parameter systems, active disturbance rejection control, event-triggered control, and adaptive control, with applications in cable-driven mechanisms.



**Miroslav Krstic** (Fellow, IEEE) received the degree (summa cum laude) in electrical engineering from University of Belgrade, Yugoslavia, in 1989, and the M.S. and Ph.D. degrees from the University of California, Santa Barbara, CA, USA, in 1992, and 1994, respectively. He is a Distinguished Professor of mechanical and aerospace engineering, holds the Alspach Endowed Chair, and is the founding Director of the Cymer Center for Control Systems and Dynamics at UC San Diego (UCSD). He is a Senior Associate Vice-Chancellor for Research with UCSD.

Prof. Krstic won the UC Santa Barbara Best Dissertation Award and Student Best Paper awards at CDC and ACC. He has been elected Fellow of seven scientific societies - IFAC, ASME, SIAM, AAAS, IET (U.K.), and AIAA (Assoc. Fellow) - and as a Foreign Member of the Serbian Academy of Sciences and Arts and of the Academy of Engineering of Serbia. He was the recipient of the SIAM Reid Prize, ASME Oldenburger Medal, Nyquist Lecture Prize, Paynter Outstanding Investigator Award, Ragazzini Education Award, IFAC Nonlinear Control Systems Award, Chestnut Textbook Prize, Control Systems Society Distinguished Member Award, the PECASE, NSF Career, and ONR Young Investigator awards, the Schuck ("96 and '19") and Axelby paper prizes, and the first UCSD Research Award given to an engineer. He has also been awarded the Springer Visiting Professorship at UC Berkeley, the Distinguished Visiting Fellowship of the Royal Academy of Engineering, and the Invitation Fellowship of the Japan Society for the Promotion of Science. He is an Editor-in-Chief of *Systems and Control Letters* and has been serving as Senior Editor in *Automatica* and *IEEE TRANSACTIONS ON AUTOMATIC CONTROL*, as Editor of two Springer book series, and was a Vice-President for Technical Activities of the IEEE Control Systems Society and as Chair of the IEEE CSS Fellow Committee. He has coauthored 13 books on adaptive, nonlinear, and stochastic control, extremum seeking, control of PDE systems including turbulent flows, and control of delay systems.